

I give permission for public access to my thesis and for any copying to be done at the discretion of the archives' librarian and/or the College library.

Kathryn Patricia Krueger
Signature

05/11/2011
Date

GLYCOPROTEIN BIOGENESIS: OPTIMIZATION OF N-
ACETYLGLUCOSAMINIDASE, LYSOSOMAL NEURAMINIDASE, AND
PROTECTIVE PROTEIN CATHEPSIN A EXPRESSION

BY:

KATHRYN PATRICIA KRUEGER

A Paper Presented to the
Faculty of Mount Holyoke College in
Partial Fulfillment of the Requirements for
the Degree of Bachelor of Arts
with Honor

Department of Biochemistry

South Hadley, MA 01075

May 2011

This thesis was prepared under the direction of

Professors of Biochemistry

Scott Garman and Craig Woodard

for eight credits.

*To my sister, Rachel, who always keeps me on my toes and to my ever-inspiring
family.*

ACKNOWLEDGEMENTS

To Professor Scott Garman for allowing me the unique opportunity to work in a graduate crystallography laboratory as an undergrad. You have been a wonderful role model and advisor throughout my time in your lab.

To Professor Craig Woodard, who has been a font of wisdom throughout the production of this document, and for his invaluable advice and unwavering support.

To Nilima Kolli, for training me and tolerating my endless stream of questions. You are a generous scientist and patient soul. To the Garman Lab: Yady, Emily, Chelsea, Matt, Cassidy, Nat, and Yurie for helping me at every turn.

To Professor Sarah Bacon for introducing me to laboratory work, and to the beauty of scientific research.

To the Mount Holyoke College faculty, staff, and students for making me a stronger person than I once believed possible, and for funding my research through a Mount Holyoke College Summer research grant.

TABLE OF CONTENTS

	PAGE
ABSTRACT	1
INTRODUCTION	
LYSOSOMAL STORAGE DISORDERS – AN OVERVIEW	3
A CLINICAL PERSPECTIVE ON LSDS	4
MACROMOLECULAR DEGRADATION	10
α -GAL – A WELL CHARACTERIZED LSD	15
REACHING A BIOCHEMICAL UNDERSTANDING OF LSDS	28
GOALS AND SCOPE OF RESEARCH	35
MATERIALS AND METHODS	
NAGLU MUTAGENESIS	36
PPCA MUTAGENESIS	37
NEU1 BACULOVIRUS EXPRESSION	40
CELL CULTURE	40
VIRAL AMPLIFICATION	41
PROTEIN EXPRESSION	41
CEDEX DATA COLLECTION	42
WESTERN BLOTTING	42
SMALL POLYCLONAL CELL LINES	43
RESULTS	
NAGLU MUTAGENESIS	48
PPCA MUTAGENESIS AND STABLE CELL LINE	53

VIRAL AMPLIFICATION OF NEU1	59
PREDICTED FOLDING	68
DISCUSSION	71
REFERENCES	80

FIGURES AND TABLES

FIGURES

	PAGE
INTRODUCTION AND METHODS	
1. The signaling cascade leading to increased stroke risk in Fabry disease patients.	8
2. The cross section of a heart of a Fabry disease sufferer.	9
3. Misfolded LSD-related enzyme degradation	12
4. The trafficking and processing of biomolecules into the lysosome	13
5. Lysosomal Catabolism	14
6. A model for LSDs and their pathology.	15
7. Human α -GAL	18
8. α -GAL mechanism	20
9. The electron density of the α -GAL substrate in the active site	21
10. Amino acid point mutations that lead to Fabry disease	23
11. Enzyme degradation in the presence of a pharmacological chaperone.	25
12. The role of pharmacological chaperones	27
13. A model proposed for the interaction between NEU1 and PPCA	31
14. A model of cellular trafficking of the lysosomal complex	32
15. The crystal structure of PPCA	34

16. The design of a bacmid leading to recombinant baculovirus	44
17. A method for developing a recombinant baculovirus for protein expression	45
18. A chart of the process of baculovirus protein expression	46
19. Signs of insect cell infection	47

RESULTS

20. PCR amplification of the gene of interest over a temperature gradient.	49
21. Gel Image of the gel electrophoresis purification	50
22. Gel Image of the <i>Xho</i> 1 digestion	51
23. Diagram of NAGLU gene and primers	52
24. Gel Image of the PCR products of a test of mutagenesis primers	53
25. Gel Image of the PCR amplification of the PPCA R284A mutation over a temperature gradient	54
26. PPCA triple mutant transfection	55
27. Western blot of baculovirus transfection	56
28. Immunodot blot showing protein production of PPCA triple mutants	57
29. Immunodot blots of PPCA and NEU1	58
30. Western Blot of viral Tn5 infection supernatant	60
31. Western blot of human Neu1 viral expression in two-year-old inoculum	61
32. Western blot of viral infection	62

33. Western blot of protein supernatant	63
34. Five generations of Sf-9 cell amplification and Tn5 expression	64
35. Viable cell density of each Tn-5 cell infection	65
36. Cell diameter in microns of each Tn-5 cell infection	66
37. Neu1 infection of Tn5 cells – Western blot	67
38. Disorder probability in human NAGLU	68
39. Disorder probability in human NEU1	69
40. Disorder probability in human PPCA	70

TABLES

	PAGE
1. NAGLU primer design	37
2. PPCA primer design	39

ABSTRACT

Humans depend on lysosomal enzymes for proper macromolecular degradation. In their absence, lysosomal catabolism is impaired, leading to Lysosomal Storage Diseases (LSDs) (Meikle, 2003). LSDs are characterized by accumulations of metabolic intermediates (Meikle, 2003; Meikle et al., 1999). Accumulation of these biomolecules over time can lead to irreversible arterial blockage, nervous tissue damage, and progressive neurodegeneration (Meikle, 2003; Naganawa et al., 2000). Most LSDs are incurable (Neufeld et al., 1975). Determining the structure of functional lysosomal enzymes is the first step toward understanding LSDs. X-ray crystallography is one technique used to understand protein structure. To perform crystallography, researchers must generate enough protein for crystallization.

Using a small polyclonal lepidopteran stable cell line, I have generated two enzymes - Protective Protein Cathepsin A (PPCA), and Lysosomal Neuraminidase 1 (NEU1). Stable cell line generation entails introduction of recombinant protein coding genes into lepidopteran cells, selecting the best protein producers through antibiotic resistance and protein immunodot blot assays. I also employed a baculovirus expression system to generate NEU1 (O'Reilly et al., 1994). Further work would include protein purification and crystallization of proteins produced. This

work has long-range applications in the rational design of small molecules that stabilize native state protein conformations (Fan and Ishii, 2007a).

INTRODUCTION

Lysosomal Storage Disorders – An Overview

Lysosomal storage disorders (LSDs) are a class of diseases characterized by molecular mechanisms: loss of activity in a critical catabolic enzyme in the lysosome. In the absence of enzymatic activity, substrates accumulate, leading to a variety of symptoms and eventually death. LSDs include Tay-Sachs disease, Fabry disease, Sanfilippo syndrome, sialidosis, galactosialidosis, and many others. While each disorder differs in gross morphology, they share similar mechanisms on a biochemical level.

We can understand LSDs through many lenses, from gross physiology to molecular mechanism. In this work, I attempt to chronicle the role that certain macromolecules play in these diseases from perspectives that often cross the lines from one discipline to the next: first from a clinical and physiological perspective, then on the cellular level. Then, to illustrate LSD genetics, structure, and biochemistry, I survey α -galactosidase, (α -GAL), the enzyme responsible for Fabry disease, in molecular detail, a perspective accessible mainly through its crystal structure, a source of information unavailable for most LSDs.

The example of α -GAL allows the reader to trace Fabry disease from a gene mutation to protein instability, plaque formation inside cells, and

clinical pathology, and design of pharmaceuticals. Such a thorough understanding of disease causation is rarely available, let alone affordable.

The missing enzymes responsible for the LSDs studied in this work, sialidosis, galactosialidosis, and Sanfilippo syndrome, have not yet been crystalized, though their biochemical functions have been studied. A thorough understanding of these enzymes' biochemistry and trafficking is essential to my attempted structural characterizations. Structural studies of PPCA, in particular, add further understanding to my work.

To provide a deep understanding LSDs, one must understand them not only through their disease pathology, but also through their molecular underpinnings.

A Clinical Perspective on LSDs

Sialidosis

There are two different clinical classifications of sialidosis: type I and type II. Type I sialidosis, the mild manifestation, displays in the second decade of life, and is typified by few infantile symptoms, while type II sialidosis manifests severe symptoms beginning in infancy. Manifestations of type I sialidosis include ocular cherry red spots, known as "cherry-red-spot-myoclonus," lenticular eye opacities (white spots on the eyes), seizures, proteinuria (protein in urine), and hypotonia (muscle weakness) (Royce and Steinmann, 2002; Swallow et al., 1979; Naganawa et al., 2000; Kashtan et al., 1989). Type II sialidosis is characterized by coarse facies

(rough facial features), developmental delays, short stature, hepatomegaly (enlarged liver), red spots on skin, splenomegaly (enlarged spleen), lens opacities, and sometimes stillbirth (Royce and Steinmann, 2002; Winter et al., 1980; Tobimatsu et al., 1985; Gravel et al., 1979). As development proceeds, symptoms of types I and II include various forms of mental retardation (Royce and Steinmann, 2002; Harzer et al., 1986).

Galactosialidosis

There are three distinct phenotypic subtypes of galactosialidosis: early infantile, late infantile, and juvenal/adult (Sons, 2002). Infants suffering from early infantile galactosialidosis are unlikely to live much past two years, while those suffering from late infantile galactosialidosis are unlikely to reach puberty. Those with juvenal/adult forms of galactosialidosis commonly live to middle age. All forms of galactosialidosis result in the accumulation of sialyloligosaccharides in the lysosome and in excreted bodily fluids (Sons, 2002).

Symptoms of galactosialidosis include edema, enlarged organs, corneal clouding, seizures and convulsions, and spinal malformation, among many others (Royce and Steinmann, 2002). For the most part, galactosialidosis symptoms overlap with those of sialidosis, though neurologic involvement is often much milder in galactosialidosis patients (Sons, 2002).

Sanfilippo Syndrome

Symptoms of the Sanfilippo syndrome include hepatosplenomegaly, aggressive hyperactivity, distorted facial features, joint stiffness, seizures, and hearing loss. Retardation may prove minimal or nonexistent early in the patient's life, but becomes more pronounced by the age of ten. Around ten, neurologic degeneration becomes more pronounced, leading to dementia and hyperactivity in the teens and twenties. Death follows neurologic degeneration, usually occurring by the mid twenties.

Fabry Disease

One of every forty thousand males born in the United States suffers from reduced amounts of functional alpha galactosidase (α -GAL) function, known as Fabry disease, a rare genetic disorder that results from the accumulation of GB3 and other substrates (Siamopoulos, 2004). GB3 causes the symptoms and physical manifestations with many systemic effects, categorized collectively as Fabry disease. Due to the wide variety of mutation types in α -GAL that can lead to Fabry disease, the symptoms of the disease vary widely depending on degree of enzymatic functionality.

Most affected individuals exhibit certain physical characteristics, such as a broad bulbous nose, sloping forehead, and large forehead slanting ears. Significant accumulation of α -GAL's substrate, GB3, must occur before the symptoms of the disease can become evident.

Consequently, Fabry disease often remains undiagnosed until GB3

buildup reaches a critical threshold, an event that often does not occur until the late teenage years, depending on their relative *GLA* mutation (MacDermot et al., 2001a). The first signs of Fabry disease usually consist of pain in the extremities, known as acroparasthesia, which is caused by GB3 destruction of small nerve endings (MacDermot et al., 2001b). These acroparasthetic GB3 accumulations near nerve endings, in addition to causing episodic pain, will eventually lead to loss of functional nerve endings, and therefore sensitivity (MacDermot et al., 2001c). Extremity pain and the appearance of small purple spots of broken blood vessels near the surface of the skin, known as angiokeratomas, are often the first observable symptoms of Fabry disease (MacDermot and MacDermot, 2001).

Accumulations surrounding nearby sweat glands will block release of sweat, leading Fabry disease suffers to be particularly sensitive to heat (Brady and Schiffmann, 2000). Similar GB3 blockages of tear ducts and salivary glands can lead to a significant decrease in tear and saliva production in some, but not all, patients (Schiffmann et al., 2001). The inability to process GB3 may lead to pain when digesting food and possibly diarrhea (Badash, 2009). GB3 accretions in the eye can lead to the equivalent of early-forming cataracts (Badash, 2009).

More serious, and often fatal, complications of Fabry disease result from GB3 accumulation in the cardiovascular system and kidneys. Deposits of GB3 in blood vessels cause symptoms that greatly resemble

cases of hypercholesterolemia and arterial hypertension shown in figure 1 below (Schiffmann, 2009).

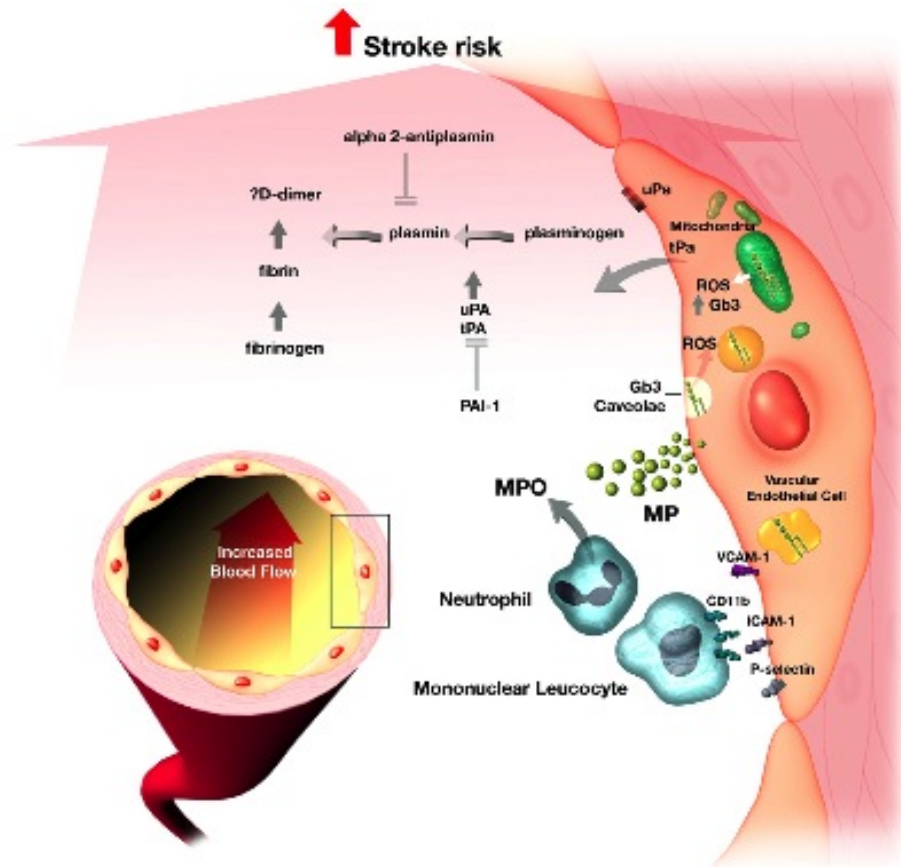


Figure 1 – The signaling cascade leading to increased stroke risk in Fabry disease patients. Accumulation of GB3 leads to the production and activation of immune cells (Schiffman, 2009).

This resemblance is due in part to the inflammatory nature of Fabry disease, since GB3 accumulations cause a release of reactive oxygen species (Schiffmann, 2009). Reactive oxygen species in turn lead

endothelial cells to release microparticles and cause the blood vessel to become much more prone to blood clotting, and strokes.

GB3 and lipid buildup in the heart can lead to a number of problems as well, forming much more rapidly and densely than the cholesterol plaques that develop in the cases of most standard atherosclerotic patients (Schiffmann, 2009). Plaques often lead to heart attacks, or in advanced cases, heart failure. Often, however, kidney failure precedes heart failure.



Figure 2– The cross section of a heart of a Fabry disease sufferer. The left ventricle contains two inches of GB3 accumulation, which can lead to heart failure (Schiffman 2009).

One of the most common symptoms of Fabry disease is proteinuria, the presence of protein in a sufferer's urine (MacDermot and MacDermot, 2001). While proteinuria does not seem like a particularly dangerous affliction, it signals that a patient's kidneys are failing. Kidney failure causes the improper filtering of blood throughout the body and leads to the accumulation of toxins in the body. In Fabry disease, kidney failure results from GB3 becoming stuck within the glomeruli and loops of Henle the filtering apparatus of the kidneys (MacDermot et al., 2001a). These accumulations lead to reduced filtration in the kidney and ultimately loss of kidney function. Eventually, this condition will lead to deadly toxin buildup in the bloodstream.

Macromolecular Degradation

Macromolecules in the cell are subject to degradation at the end of their lifespan. When a protein is misfolded, it is subject to degradation upon formation, or upon lack of functional stability. Both types of degradation can occur in LSDs. Mutant enzymes are degraded in the ER lumen through the ERAD system, which leads to their polyubiquitination and subsequent degradation by the 26S proteasome. The Unfolded Protein Response (UPR) may also play a role in the enzyme degradation characteristic of LSDs, though a firm connection between the UPR and LSD-related enzyme degradation has not yet been established. If

misfolding is less pronounced, these enzymes are trafficked to the lysosome where they are degraded. Disease symptoms may emerge in part due to altered formation of autophagosomes, and to impairment of autophagosome-lysosome fusion, which impedes autophagy (Settembre et al., 2008). This impeded autophagy can lead to the accumulation of substrates, which appears a common pathogenic mechanism across many LSDs (Settembre et al., 2008).

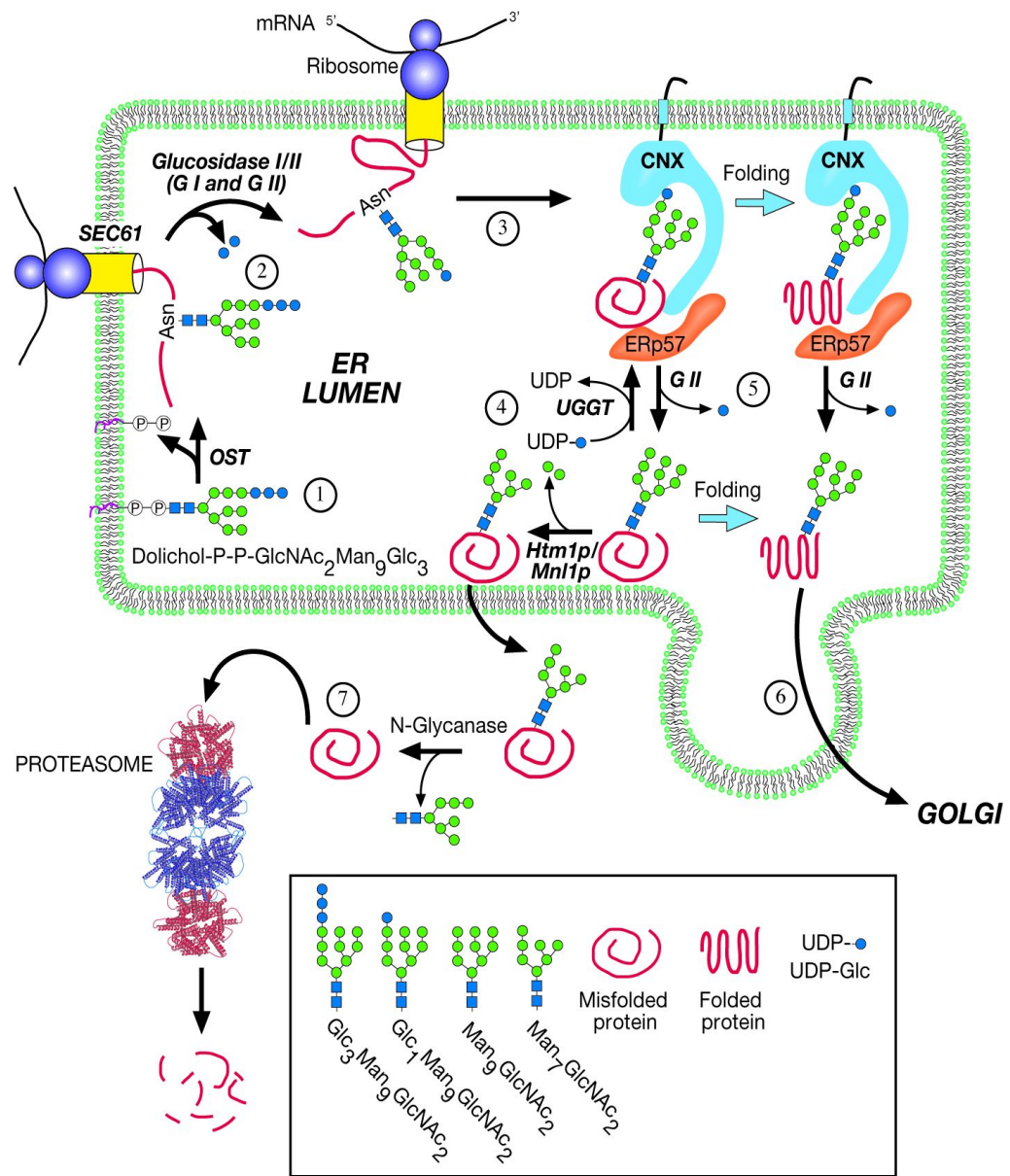


Figure 3 – Misfolded LSD-related enzymes are degraded through the 26S proteasome, or trafficked to the lysosome by virtue of mannose-6-phosphate receptors. In the lysosome they are degraded through autophagy (Varki, 1999).

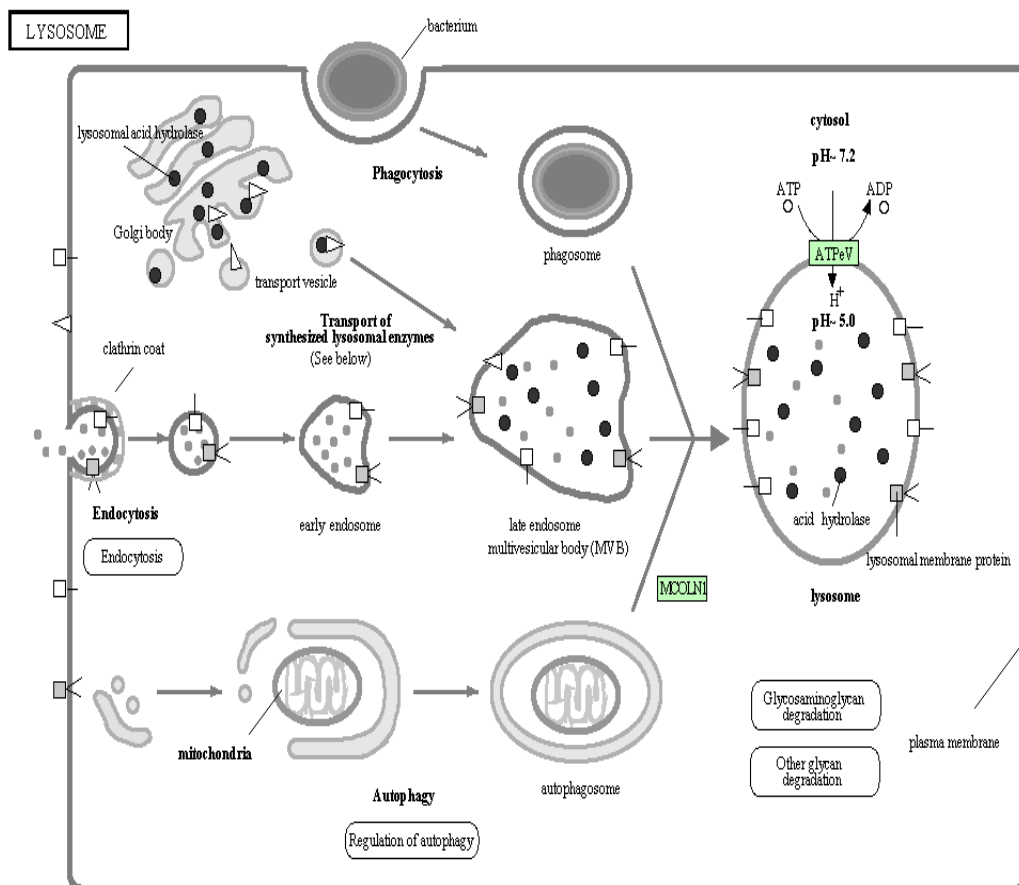


Figure 4 – The trafficking and processing of biomolecules in the cell, from their entry via phagocytosis to their transit into the lysosome. Inside the lysosome, these molecules are processed by a wide variety of lysosomal catabolic enzymes (Kanehisa et al., 2010)

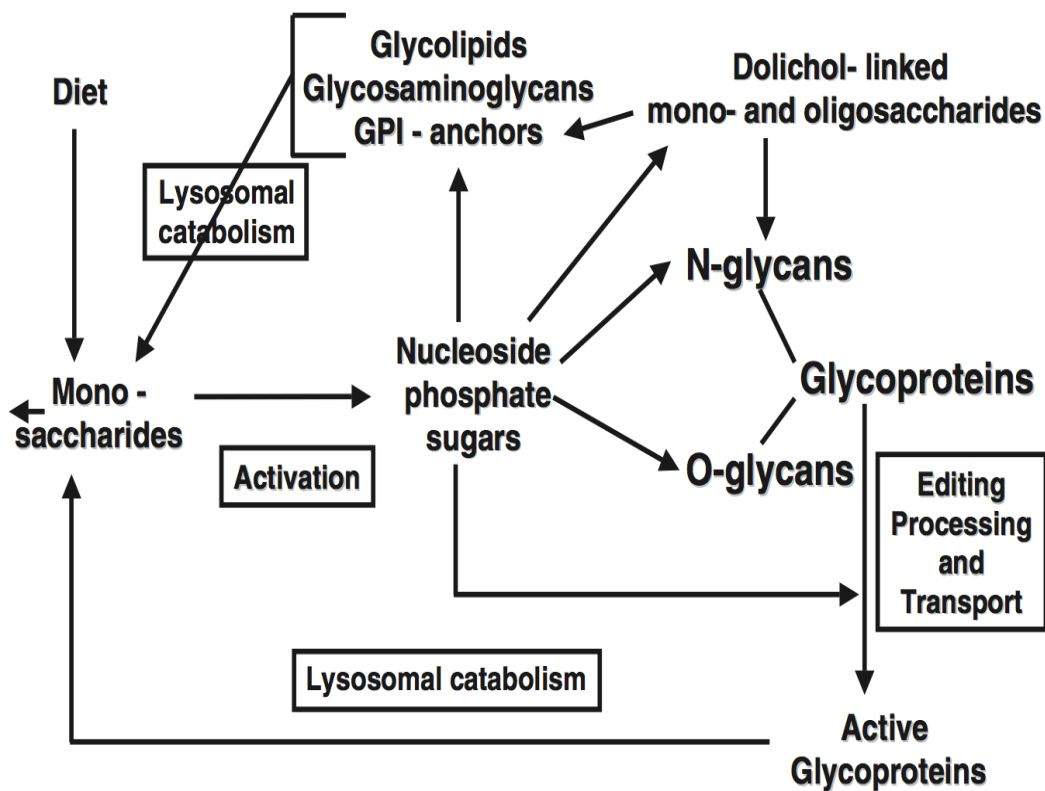


Figure 5- Lysosomal Catabolism – The lysosome is the center of a plethora of catabolic activities. It is also the final destination of some Golgi-derived glycoproteins, such as those implicated in lysosomal storage disorders (Winchester B., 2005).

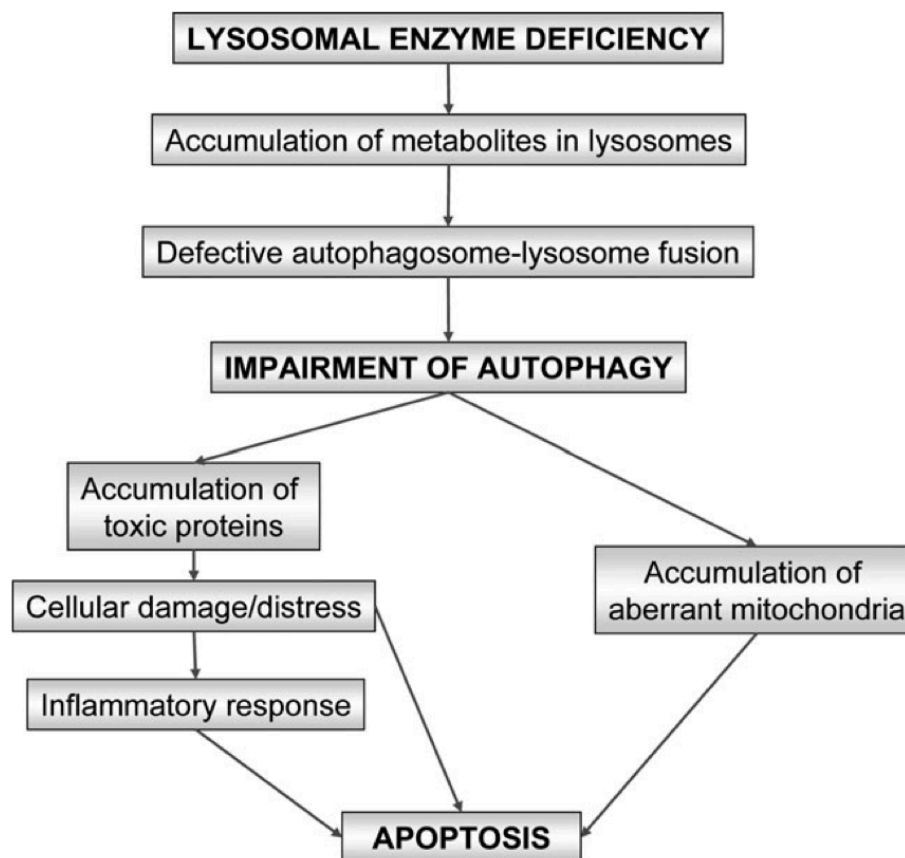


Figure 6– A model for LSDs and their pathology. While some LSDs may result from mutations that occur prior to the trafficking to the lysosome, many result from this mechanism (Settembre et al., 2008).

Fabry Disease – A Well Characterized LSD

To provide further insight into the role of LSD-linked glycoproteins in the catabolic processes of the cell, it is useful to examine the research performed on α -galactosidase (α -GAL). The lysosomal

enzyme α -GAL has been extensively studied, and its crystal structure has been solved (Garman and Garboczi, 2004). Treatment of Fabry disease, the deficiency of properly folded α -GAL has come to include pharmacological chaperones, which may prove critical in therapies targeted at other LSDs as well (Fan and Ishii, 2007b; Guce et al., 2010a).

Genetics

Fabry disease is an X-linked disorder with intermediate penetrance in women; the *GLA* gene is located on the X chromosome (Bishop et al., 1988). Much of the research on α -GAL today centers on managing Fabry disease by lowering the impact of damaged α -GAL proteins in affected individuals. Such techniques include the formation of protein stabilizing molecules known as chaperones (Fan and Ishii, 2007b).

Most of the mutations in the coding region for the α -GAL gene are missense mutations (mutations that code for different amino acids than those typically specified) or nonsense mutations (mutations that code for a premature “stop” codon, terminating amino acid synthesis). The majority of these mutations result in the improper folding of the α -GAL enzyme. These misfolded proteins may retain most of their function, but will degrade much more rapidly over time than properly folded proteins (Henrissat and Davies, 1997).

The gene that codes for functional α -GAL protein is located on the X-chromosome (Ishii et al., 2007). This location means that men experience the severe form of Fabry disease at a much higher frequency than do

women because men have only one X-chromosome (Schiffmann, 2009). Women exhibit a wider range of Fabry disease symptoms if they have two mutant forms of *GLA* (Wang et al., 2007a). More frequently, women are heterozygous for the mutant alleles of the gene that causes Fabry disease (Wang et al., 2007a). One mutant copy of the *GLA* gene leads to various degrees of Fabry disease, since random X-inactivation occurs in *GLA* mutations, leading to a wide variety of phenotypes. Thus, the effects of abnormal α -GAL in heterozygous women vary from extremely mild cases with few symptoms to those that are more classically male (Wang et al., 2007a). In general, Fabry disease in women is still largely underdiagnosed.

The *GLA* gene sequence contains seven exons (Yan, 2009). The 398 amino acids of α -GAL protein are coded for by 1194 nucleotides (Bishop et al., 1988). The *GLA* gene also contains a region of DNA that codes for a 31-amino acid signal peptide (Wang et al., 2007b). In total, 431 mutations in the gene coding for α -GAL have been recognized and characterized (Schiffmann, 2009). The majority of these mutations are missense and nonsense mutations, while insertions and deletions are much less common (Schiffmann, 2009).

Structure

The structure of human α -GAL has been solved to the resolution of 3.25 Angstroms (Garman and Garboczi, 2004). This degree of resolution provides information about the overall organization of the protein and its

domains as well as information about the location of amino acids.

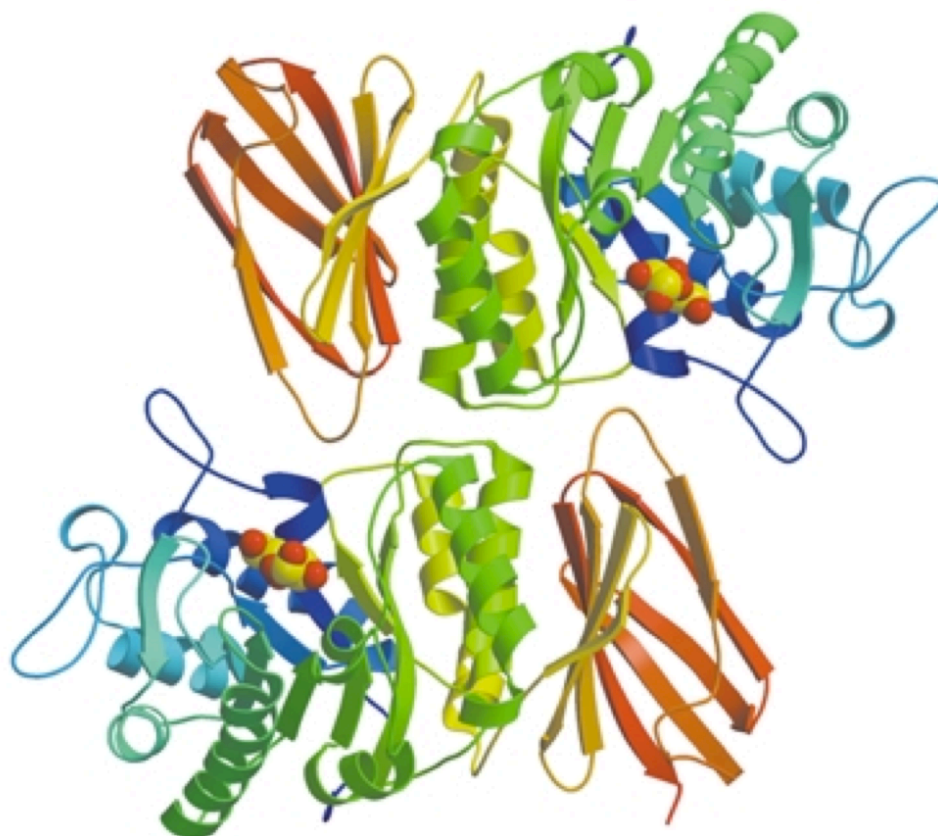


Figure 7 – The 3.25 Å resolution crystal structure of human α -GAL colored in gradations from blue at the N-terminus to red at the C-terminus (Garman and Garboczi 2004).

Human α -GAL removes a terminal six carbon sugar unit from its substrate without changing the configuration of the anomeric carbon (Henrissat and Davies, 1997). Thus, it is classified as a retaining exoglycosidase from family 27 (Henrissat and Davies, 1997). Functional α -

GAL is a homodimer, and contains 398 residues per monomer (Garman and Garboczi, 2002).

Human α -GAL is composed of two identical monomers (see figure 7) (Garman and Garboczi, 2002). Each of these monomers, in turn, contains two domains. Domain 1 contains the enzyme's active site where catalysis occurs, while domain 2 contains the C-terminus region consisting of antiparallel beta strands and in the form of a sandwich whose function has not yet been determined (Fujimoto et al., 2003; Garman and Garboczi, 2002). The active site is nestled within the center of a domain 1 beta barrel. (Garman and Garboczi, 2002). Each monomer contains five disulfide bonds that stabilize the protein.

The enzyme consists of an $(\beta/\alpha)_8$ domain extending from amino acid 32 to 332, and a beta domain extending from amino acid 333-429. Twelve residues at the center of the beta barrel in the $(\beta/\alpha)_8$ domain comprise the active site, and these residues are conserved among many galactosidases across species (Garman and Garboczi, 2002).

While some of the amino acid sequence of the human α -GAL clan are conserved, the general fold and active site structure is highly conserved. All members have antiparallel beta sheets as part of their second domain, and possess a $(\beta/\alpha)_8$ barrel in their first domain (Fujimoto et al., 2003). Twelve amino acids from the active sites of these enzymes (two involved in catalysis and ten involved in structure) are conserved across clan members (Garman and Garboczi, 2004) .

Kinetics and Mechanism

Recent crystallographic studies have allowed for a more thorough understanding of the catalytic mechanism of α -GAL (Guce et al., 2010b). By using a difluoro- α -galactopyranoside compound, Guce and colleagues were able to capture the intermediate structure of human α -GAL (2010). Structures containing difluoro- α -galactopyranoside intermediates have allowed a more comprehensive understanding of the exact mechanism of catalysis, which involves the ligand acquiring a skew boat conformation (Guce et al., 2010b).

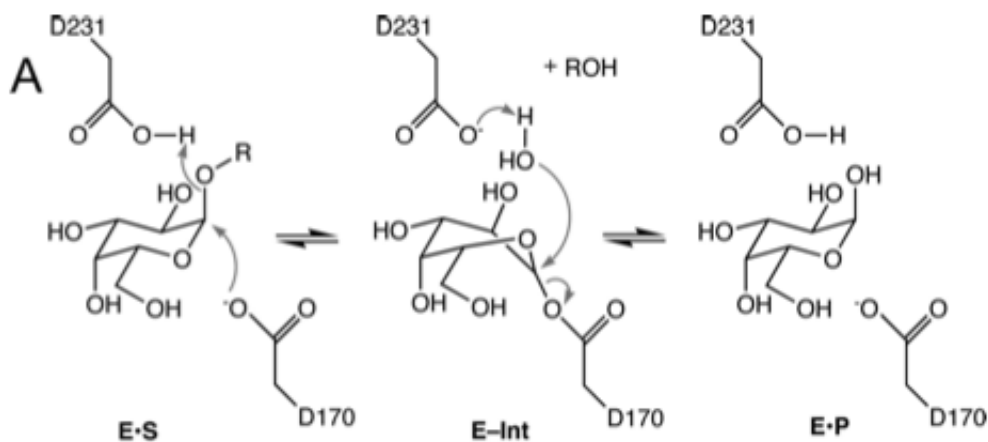


Figure 8– The α -GAL reaction mechanism (Guce et al., 2010b). This mechanism shows that the ligand is twisted into a skew boat conformation in course of each reaction.

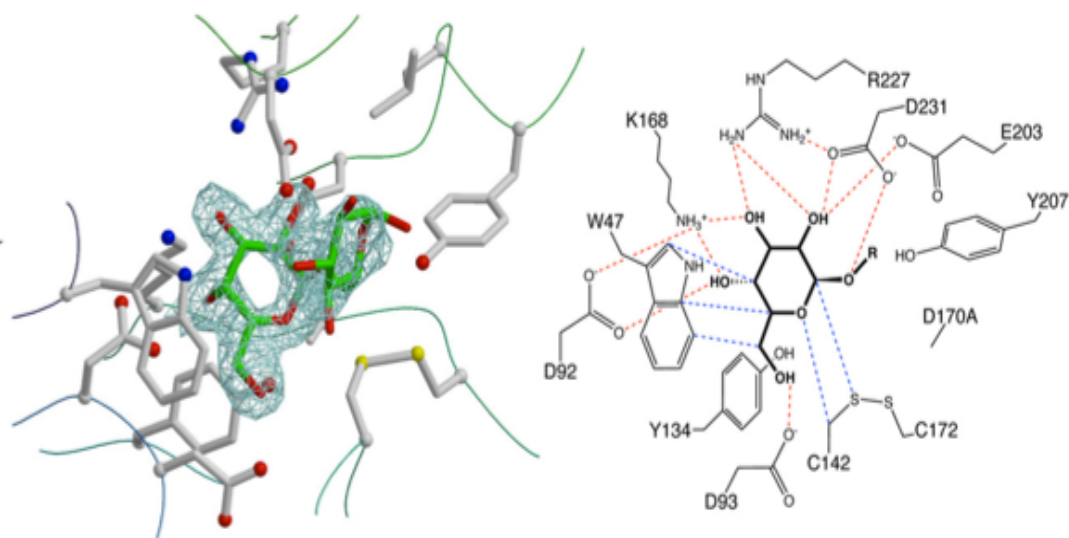


Figure 9– The electron density of the α -GAL substrate in the active site. The figure at left shows the electron density of the substrate in the active site, while the figure at right shows the hydrogen bonds in red and the van der Waals interactions in blue (Guce et al., 2010b).

Mutations that Lead to Disease

Garman and colleagues have amassed an exhaustive list of amino acid mutations leading to Fabry disease (Garman and Garboczi, 2004). In total, they have classified over three hundred different varieties of Fabry disease by amino acid mutation (Shabbeer et al., 2006). These mutations are entirely single point mutations, mainly deletions or substitutions, yielding isolated mutations that allow for a better understanding of how changes in amino acids correspond to α -GAL function in Fabry disease patients (Garman and Garboczi, 2004).

The majority of the mutations leading to Fabry disease occur in domain 1 of the protein, where they affect the folding of the enzyme. These tend to lead to severe manifestations of Fabry disease with an earlier onset. Functionally, most of these mutations are in the protein's hydrophobic core. Sometimes, mutations near the active site may dramatically change the phi-psi angles (protein fold configuration) near the active site, inhibiting substrate entry into the enzyme. In some cases, these mutations eliminate α -GAL function altogether (Garman and Garboczi, 2004).

Mutations in domain 2, much farther from the active site, often involve damage to α -GAL's hydrophobic core or alter the protein's general structural integrity.

Enzyme Replacement Therapy

Within the past twenty years, the fate of Fabry disease patients has become much less grim. Insights gained through structural and kinetic studies of α -GAL have allowed scientists to create a number of large and small molecule therapeutic agents. One therapy, enzyme therapy, was approved by the FDA in 2003, and chaperone therapy is currently in Phase 3 clinical trials. At present, these therapies are the most powerful treatments for Fabry disease available to patients. Both treatment methods have significant drawbacks.

Human Sequence	Fabry Mutation/ (Cardiac)	Importance in α -GAL	Side Chain Access. Surface Area (\AA^2)	Point Mutation Category	Reference
1	M I	AUG start		Other	Blanch (1996) Hum Mutat 8, 38 Eng (1997) Mol Med 3, 174 Shabbeer (2002) Mol Genet Metab 76, 23
14	L P	in signal sequence		Other	Tse (2003) Nephrol Dial Transplant 18, 182
20	A (P)	in signal sequence		Other	Nakao (1995) N Engl J Med 333, 288
31	A V	in signal sequence		Other	Eng (1997) Mol Med 3, 174
32	L P	signal sequence cleavage site	7.1	Other	Madsen (1995) Hum Mutat 5, 277
34	N S	bifurcated H-bond to N224	1.7	Buried	Eng (1993) Am J Hum Genet 53, 1186
35	G R	Gly phi/psi, Arg collides with N192 carbohydrate	6.3	Other	Davies (1994) Hum Mol Genet 3, 667
40	P S	helix terminus, buried and packed on W262	0.0	Buried	Koide (1990) FEBS Lett 259, 353 Ashton-Prolla (2000) J Investig Med 48, 227
42	M V	buried, no room for beta branch	0.7	Buried	Davies (1996) Eur J Hum Genet 4, 219 Shabbeer (2002) Mol Genet Metab 76, 23
43	G D	no room for side chain	0.0	Buried	Shabbeer (2002) Mol Genet Metab 76, 23 Shabbeer (2002) Mol Genet Metab 76, 23 Germain (2002) Mol Med 8, 306
44	W X	stop	0.0	-	Sakuraba (1990) Am J Hum Genet 47, 784
45	L R	little room for a buried charge	2.4	Buried	Eng (1997) Mol Med 3, 174
46	H R	buried, next to W47 in active site	0.0	Buried	Eng (1997) Mol Med 3, 174 Eng (1997) Mol Med 3, 174 Blaydon (2001) Hum Mutat 18, 459
47	W G	active site residue	3.8	Active	Blaydon (2001) Hum Mutat 18, 459
49	R L	mostly buried, on dimer interface	2.9	Buried	Davies (1994) Hum Mol Genet 3, 667 Davies (1996) Eur J Hum Genet 4, 219 Blaydon (2001) Hum Mutat 18, 459 Germain (2002) Mol Med 8, 306
50	F C	buried in hydrophobic pocket	0.4	Buried	Shabbeer (2002) Mol Genet Metab 76, 23
51	M K	contacts to active site W47 and dimer interface	14.7	Active	Ashley (2001) J Hum Genet 46, 192
52	C S	disulfide required near active site	13.0	Other	Eng (1994) Hum Mol Genet 3, 1795 Blanch (1996) Hum Mutat 8, 38 Topaloglu (1999) Mol Med 5, 806
56	C G	disulfide bond	10.6	Other	Eng (1993) Am J Hum Genet 53, 1186 Eng (1994) Hum Mol Genet 3, 1795 Davies (1996) Eur J Hum Genet 4, 219
59	E K	ion pairs across dimer interface to H406	7.9	Other	Eng (1994) Hum Mol Genet 3, 1795
65	S T	partially buried	3.9	Other	Chen (1998) Hum Mutat 11, 328
66	E Q	mostly buried in ion pair	3.1	Buried	Ishii (1992) Hum Genet 89, 29
68	L F	buried in hydrophobic pocket	0.6	Buried	Shabbeer (2002) Mol Genet Metab 76, 23

Figure 10 - Some of the amino acid point mutations that lead to Fabry disease. Note mutations such as Human Sequence 47, in which a switch from tryptophan to glycine directly above the enzyme's active site alters the catalytic capacity of the two catalytic aspartate residues, inhibiting their function, which is regained for ligand binding. (Garman, et al. 2004).

Enzyme replacement therapy is the only Fabry disease treatment that is able to benefit patients regardless of *GLA* mutation type. Relying on recombinant α -GAL enzyme that contains the same amino acid sequence as normal α -GAL, enzyme replacement therapy is able to increase the quality and possibly the duration of patients' lives (Desnick, 2004). Regular infusions of synthetic α -GAL allow for increased processing of GB3 that slows down the accumulation of plaques through the sufferer's body (Ferverza et al., 2008). Additionally, enzyme infusions slow the clogging of the glomeruli in the kidneys, preventing proteinuria and rapid kidney failure in patients (Ferverza et al., 2008).

While enzyme replacement therapy represents the first step towards comprehensive Fabry disease treatment, there is much room for refinement. On a practical level, enzyme replacement therapy proves challenging to provide to patients on a regular basis. Recombinant Fabrazyme injections must be given every two weeks, and Replegal injections must be given every week for the entirety of a sufferer's life. Over the course of a year these therapies cost patients or healthcare providers over \$100,000 (Wilcock, 2009).

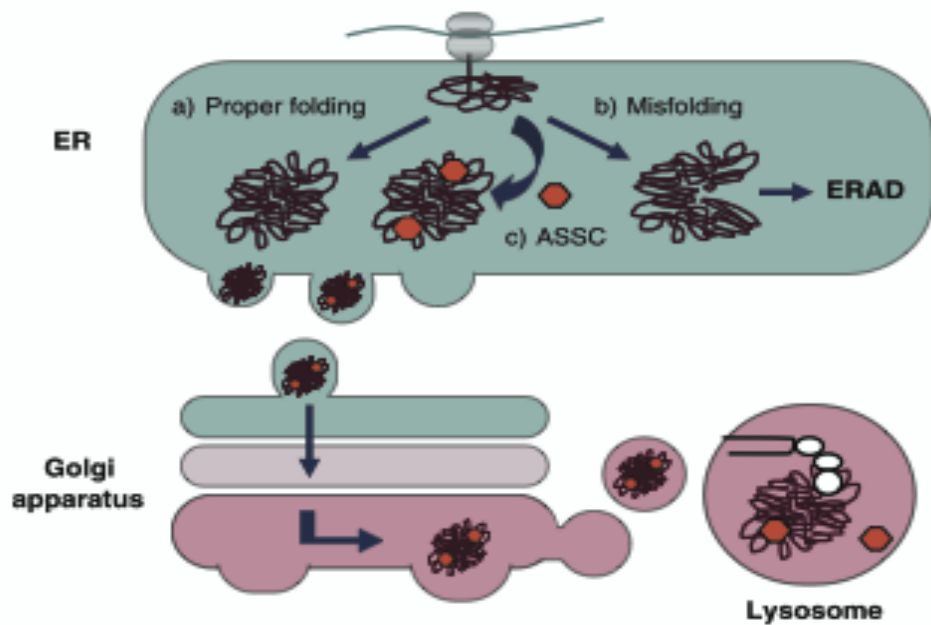


Figure 11 – Enzyme degradation in the presence of a pharmacological chaperone. Such degradation leads to an inadequate quantity of functional α -GAL. One solution is adding a pharmacological chaperone (shown in the diagram as red hexagons) (Fan et al. 2007).

Recombinant α -GAL causes a powerful immune response in nearly 80 percent of patients, which must be treated with anti-inflammatory agents (Desnick et al., 2002). In patients who are already experiencing kidney failure, artificial α -GAL may be of little to no use. Two products on the market, Fabrazyme, produced in a Chinese Hamster Ovary cell line, and Replagal, produced in a human cell line, both have the same amino acid sequence as α -GAL (Ferverenza et al., 2008).

Chaperone Therapy

Chemical Chaperone therapy (also known as pharmacological chaperone therapy or active-site specific chaperone therapy) is an approach for Fabry disease currently in Phase 3 clinical trials. It is capable of treating many of the aspects of Fabry disease without the side effects of enzyme replacement therapy. This method involves the addition of small molecules that serve as substrate analogues to stabilize α -GAL (Wilcock, 2009). Such stabilization prevents mutant misfolded forms of the enzyme from degrading prematurely and allows these mutants to retain most of their function (Desnick et al., 2002). While chaperone therapy only benefits patients with structural, rather than catalytic, mutations to α -GAL, its effect on structural α -GAL mutants is dramatic (Yam et al., 2005). In addition, as a small molecule, chaperones may be taken in pill form and are much less expensive to produce than recombinant α -GAL enzyme.

Early candidate chaperones for α -GAL have included one of the enzyme's products, galactose (Brady, 2006). This molecule has been shown to promote proper protein folding and to prevent premature degradation with few side effects. Even more effective chaperone candidates include 1-deoxygalactonojirimycin (known as DGJ), which serves as a substrate analogue, keeping α -GAL from degrading (Fan and Ishii, 2007b). Currently, DGJ is in the midst of clinical trials and may become available to Fabry disease patients in the near future (Wilcock, 2009).

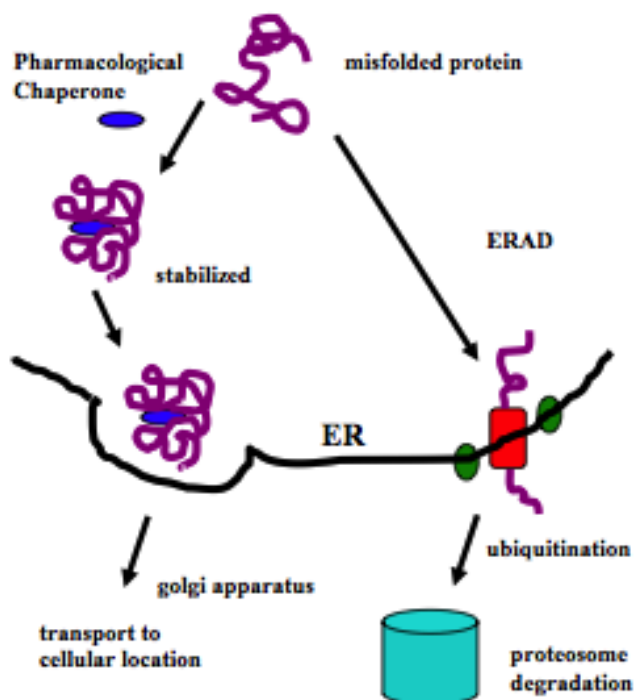


Figure 12 – The role of pharmacological chaperones in maintaining proper protein folding. Proper folding allows for protein transport and successful function (Wilcock, 2008).

While other potential therapies for Fabry disease may eventually become a reality, at present they are far from effective. Substrate reduction, which involves the addition of synthetic ceramide to the bloodstreams of Fabry disease patients, is only effective in very mild cases of Fabry disease, though it may eventually be effective if used in tandem with enzyme replacement therapy (Brady, 2006). Substrate reduction therapy has been shown to be effective in other LSDs, including Gaucher disease (Zimran 2003). Gene therapy and gene editing, techniques that could eventually allow physicians to override premature stop codons and

correct the DNA sequences that lead to the formation of the wrong amino acids (Brady, 2006), have been proposed as potential treatments. At present, however, neither method has met with any success in the treatment of Fabry disease (Brady, 2006).

Reaching a Biochemical Understanding of LSDs

Without the crystal structures of proteins implicated in LSDs, such as sialidosis, galactosialidosis, and Sanfilippo syndrome, it is challenging to understand their molecular etiologies. Biochemical studies on the structure and trafficking of these enzymes has shed light on these diseases.

Biochemistry - Sialidosis, Galactosialidosis, and Sanfilippo Syndrome

Sialidosis

Sialidosis is a recessive disease that results in the lack of sialyl cleavage in glycopeptides and oligopeptides (Royce and Steinmann, 2002; Meikle, 2003). On a biochemical level, sialidosis is characterized by inadequate amounts of lysosomal neuraminidase, the enzyme that cleaves terminal neuraminic acid from oligosaccharides during their degradation in the lysosome (Royce and Steinmann, 2002; Figura and Hasilik, 2010). Sialidosis is the direct result of oligosaccharide accumulation throughout

the body of a patient. Most accumulated oligosaccharides contain neuraminic acid linked to galactose via $\alpha(2 \rightarrow 6)$ or $\alpha(2 \rightarrow 3)$ linkages (Royce and Steinmann, 2002).

Sialidosis stems from mutations in *NEU1*, the lysosomal neuraminidase (Meikle et al., 1999). Absence of NEU1 leads to accumulation of uncleaved glycopeptides and oligopeptides in bodily tissues, leading to a wide range of degenerative symptoms (Royce and Steinmann, 2002). While there are three different neuraminidases in the human body (lysosomal, plasma membrane, and cytosolic), it has been determined that sialidosis results only from deficiencies of NEU1 (Royce and Steinmann, 2002).

Human NEU1, the enzyme responsible for sialidosis, is a heavily glycosylated 42 kDa protein (Warren, 1959). Its structure has not been determined, nor has it been cocrystallized with β -galactosidase and PPCA, though it is known that the three proteins are trafficked in a complex to the lysosome (Bonten and d'Azzo, 2000; Bonten et al., 2009a). Determining the structure of human NEU1 would allow for better characterization of the relationship between NEU1, β -galactosidase and PPCA. It would also allow for the development of chemical chaperones, molecules that stabilize mutant proteins and allow for proper protein folding and prevent premature protein degradation. Chaperone therapy has been used with some success in other LSDs, such as GM1-gangliosidosis (a deficiency of properly folded β -galactosidase) (Matsuda et al., 2003; Fan and Ishii, 2007a)

Galactosialidosis

Galactosialidosis is a LSD resulting from mutations in the *CSTA* gene on chromosome 20q13.1 leading to improper amino acids in the Protective Protein/Cathepsin A (PPCA) (Sons, 2002). Since PPCA is critical to the trafficking of Glb1 and NEU1 to the lysosome, defects in PPCA protein affect all three members of the lysosomal complex of Glb1, NEU1, and PPCA. Thus, the symptoms of galactosialidosis typically resemble those of sialidosis and GM1 gangliosidosis (an LSD characterized by defective Glb1) combined.

In all tissues, GLB1 is known to form large, multi-subunit multimers, ranging from clumps of two or three to aggregates that can weigh up to 750,000 kDa, as large, in fact, as some virus particles. Likewise, lysosomal hydrolases in general have the tendency to cluster into aggregates. There is an increasingly large body of information that suggests that aggregation of lysosomal enzymes in general regulates their catalytic activity. The complex of NEU1, PPCA, and GLB1 is no exception.

In the presence of PPCA, both NEU1 and GLB1 are trafficked by the mannose-6-phosphate receptor, using PPCA's mannose 6-phosphate glycosylation. They traffic from the endoplasmic reticulum (ER) to the Golgi apparatus and to the lysosome, where each enzyme performs its catalytic function. In the absence of PPCA, NEU1 and GLB1 are not trafficked to the lysosome.

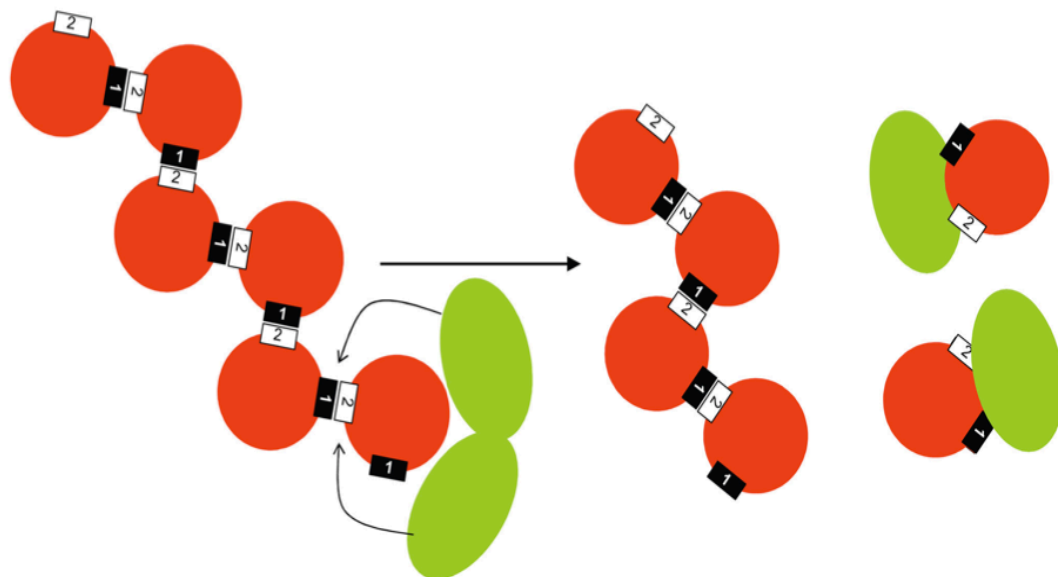


Figure 13 – A model proposed for the interaction between NEU1 and PPCA. In the absence of PPCA, Bonten et al. hypothesize that NEU1 (represented by red spheres) forms long oligomeric chains. In the presence of PPCA, however, it is believed that NEU1 forms smaller oligomers and complexes. This proposed interaction could explain in part NEU1's lack of catalytic function in the presence of catalytically functional PPCA. If NEU1 forms long chains, PPCA's functionality as a chaperone would not be dependent on its function (Bonten et al., 2009a).

GLB1 and PPCA are able to perform their respective catalytic functions.. The formation and general function of this lysosomal complex appears to be largely conserved across mammals, as it has been documented in human tissues, as well as bovine liver and porcine testes (Yamamoto and Nishimura, 1987).

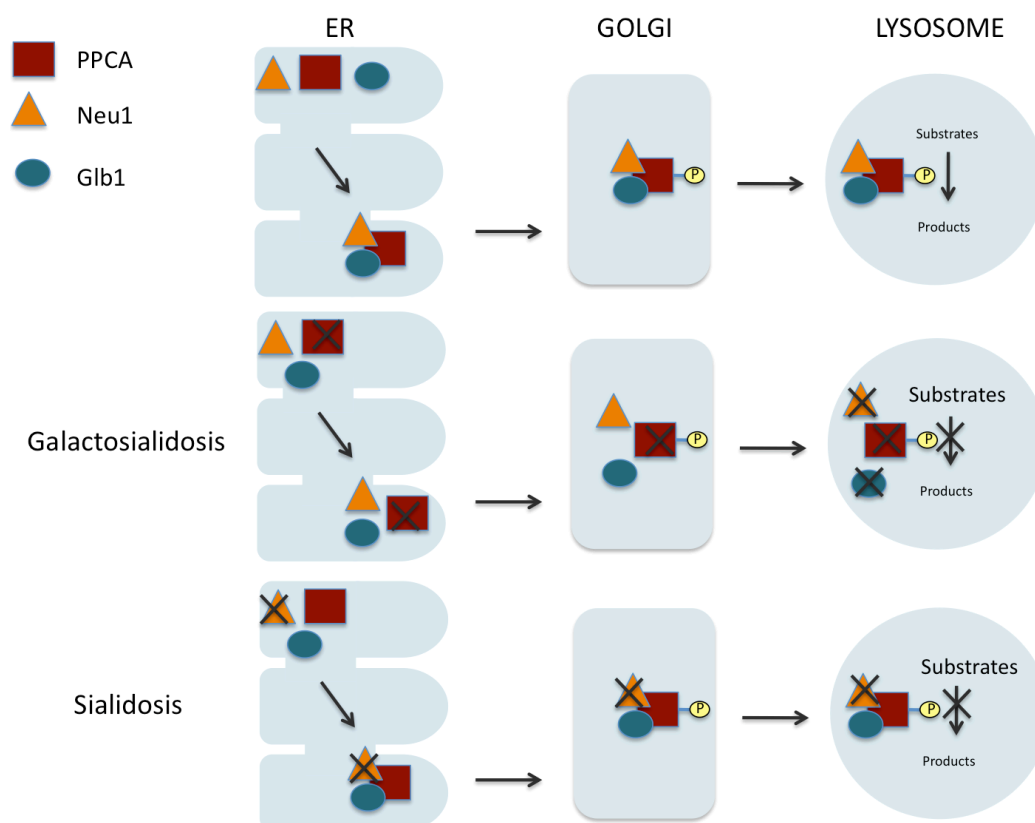


Figure 14 – A model of cellular trafficking of the lysosomal complex: protective protein/Cathepsin A (PPCA), lysosomal neuraminidase (NEU1), and beta galactosidase (Glb1). In the presence of PPCA, both NEU1 and Glb1 are trafficked (by virtue of PPCA's mannose 6-phosphate) from the endoplasmic reticulum (ER) to the Golgi apparatus and to the lysosome, where each enzyme performs its catalytic function. In the absence of catalytically functional PPCA, all enzymes are trafficked to the lysosome, but none are able to function catalytically. However, in the absence of catalytically functional NEU1, Glb1 and PPCA are able to perform their respective catalytic functions.

The lysosomal complex is not a rare species in human tissue. In fact, it constitutes 15-20% of all the GLB1 in the human placenta (Hubbes et al., 1992). An acidic pH provides the ideal conditions for the assembly of the complex, mainly by favoring the presence of monomeric GLB1. PPCA is essential for their trafficking (Figure 13) from the endoplasmic reticulum (Bonten et al., 2009b). Also, PPCA is essential for the optimal function of GLB1. In the absence of catalytically functional PPCA, insufficient function of GLB1 and NEU1 leads to a disease that encompasses both the symptoms of the entire complex, known as galactosialidosis (Bonten et al., 2009b).

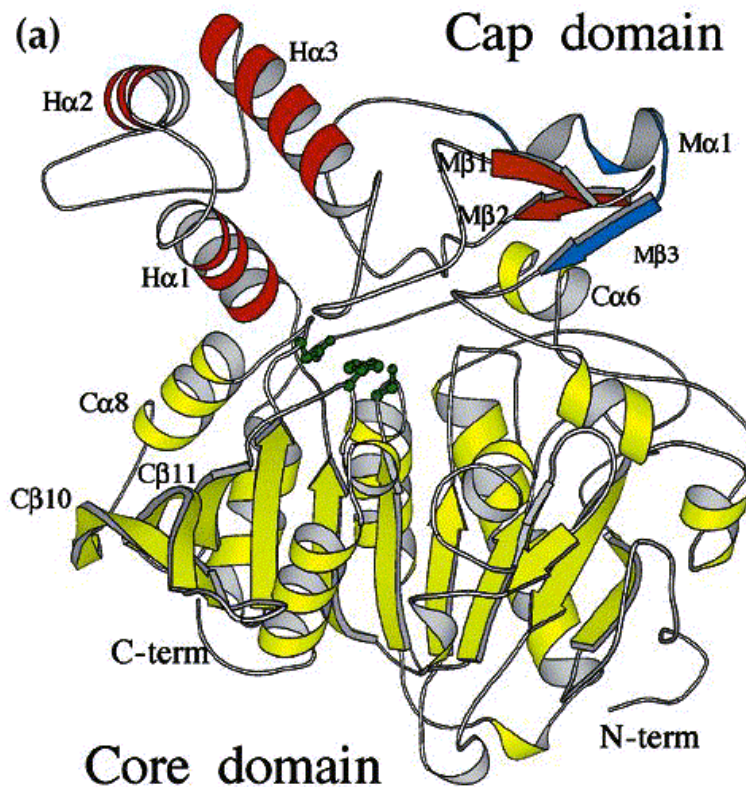


Figure 15 - The crystal structure of PPCA crystallized by the d'Azzo group in 1995. The core domain (shown in yellow) contains the catalytic triad of the serine protease: Ser150, His429, and Asp372. The excision peptide (shown in red) is only present in the immature, catalytically inactive form of the enzyme. The enzyme forms a dimer shortly after synthesis in the endoplasmic reticulum prior to the formation of the lysosomal triad of PPCA, NEU1, and Glb1 (Rudenko et al., 1995).

Sanfilippo Syndrome

Sanfilippo syndrome, also known as mucopolysaccharidosis IIIA, is an autosomal recessive genetic disorder that results in central nervous system degeneration and somatic symptoms which vary in severity according to the age of onset and type of mutation displayed in the enzyme.

Human alpha N-acetylglucosaminidase (NAGLU) is an enzyme that functions in the degradation of heparin sulfate in the lysosome. In the absence of sufficient quantities of functional NAGLU, substrate accumulates throughout the body. This accumulation is characterized as Sanfilippo syndrome type B.

Goals and Scope of Research

In this study, I attempted to create a mutant NAGLU construct for generation of a stable cell line and created a successful PPCA construct, which I introduced into *Trichoplusia ni* cells. I then created and maintained a stable cell line of NEU1 producing cells and optimized a baculovirus expression system to express human NEU1 in *Trichoplusia ni* cells (Chung et al.; Granados et al., 1994; Hsu et al., 1997). Baculovirus expression of human NEU1 will allow for enough protein to attempt crystallization, and ultimately, human NEU1 structure determination. Western blotting has been used to confirm the presence and quantity of protein produced, and

Spodoptera frugiperda cells were used to increase viral titer, through amplification infections (Wickham et al., 1992).

Since a combination of viral amplification in *Spodoptera frugiperda* cells and protein expression in *Trichoplusia ni* cells has proven an effective mechanism for producing large quantities of our proteins of interest, we anticipate generating a sufficient amount of protein for purification, and eventually crystallization.

Materials and Methods

A. NAGLU Mutagenesis

In previous experimental work, adding a polyhistidine tag (His6X) to the C-terminal end of the NAGLU protein resulted in unsuccessful protein purification. To allow for better purification, a NAGLU -streptavidin construct was designed, containing the DNA sequence encoding the Strep tag of Ala-Trp-Arg-His-Pro-Gln-Phe- Gly-Gly' at the C-terminus of the protein (Skerra and Schmidt, 1999). The 2.232 kilobase human *NAGLU* gene was PCR amplified using mutagenesis primers added the Strep tag to the construct. A Biorad MyCycler thermal cycler Model No. 580BR1658 and F530L Phusion Hot Start DNA Polymerase Lot 96 New England Biolabs were used for PCR amplification.

The subsequent product was ligated into a pIB/V5-HisTopo vector from Invitrogen featuring an OpIE2 promoter (3.5 kilobase pairs) for a size of approximately 5.7 kilobase pairs total (vector plus insert) using Ligase Fisher Scientific Part No. FP2105. The plasmid containing vector and insert was then introduced into competent Top10 cells (Invitrogen) using a standard heat shock transformation protocol and plated on LB Ampicillin plates and left overnight. Colonies were picked, restreaked, and grown overnight. Restreaked colonies were then sent to Genewiz Laboratory (Genewiz, Incorporated) for sequencing. All DNA concentrations were determined using a Nanodrop 2000c Spectrophotometer.

<i>NAGLU</i> Strep forward	AGTGCCTGGAGCCACCCGCAGTTCGAAAAATAACACCATCA CCATCACCATTAAAAGGGCAATTCTGCAG
<i>NAGLU</i> Strep reverse	GCAGCAGTGCCTGATGCCACATCCGCTTGA

Table 1 - *NAGLU* Primers [5' → 3']

B. PPCA Mutagenesis

PPCA exists in two distinct forms: an immature form containing an excision peptide, and a mature form, in which the excision peptide has

been removed. Since PPCA autocatalyzes its conversion from immature to mature forms, a solution containing wild type PPCA contains both the mature and the immature forms of the protein. It is much easier to obtain a crystal if there is only one form of PPCA present in a solution. Thus, we have rendered PPCA catalytically inactive and mutated two key residues that contribute to the enzyme's autocatalysis. To suppress maturation of the PPCA and render the enzyme catalytically inactive, we have created a mutant containing three amino acid substitutions: S150A, R284A, and R298A which prevents cleavage of the excision peptide in solution. Since this protein results from three separate amino acid substitutions in the wild type PPCA, we call it the PPCA triple mutant.

We have scaled up the top protein producers as determined by immunodot blot.

PPCA S150A forward	CTTTTCCTGACCGGGGAGGCCAAGCTGGATCTACATCCCCA
PPCA S150A reverse	TTTGTTGTTCTTGTACTCCGGAAAGAGGCGGAAGAAATCTTG AAG
PPCA R284A Forward	TCACTCGGGCCTGCCACTCAAGGCCATCTGGCATCATGGCA CTGCTGC
PPCA R284A Reverse	AGATGTTGCCCAAATCCTGGACCACAACAACAGTCTC
PPCA R298A Forward	GCTCAGGGGATAAAGTGGCCATGGACCCCCCTGCACCA
PPCA R298A Reverse	GCAGCAGTGCCTGATGCCACATCCGCTTGA

Table 2 - PPCA Primers [5' → 3']

C. NEU1 Baculovirus Expression

For production of recombinant lysosomal neuraminidase (NEU1), a recombinant baculovirus was generated. Shuttle vectors, also known as bacmids, are utilized for large-scale protein expression. The gene encoding the protein of interest is inserted into a donor plasmid, which is in turn introduced into *E. coli* cells and transposed into a bacmid. Plasmid DNA extraction yields large quantities of bacmid DNA containing the gene of interest. This DNA was subsequently introduced into insect cells through use of lipofectamine micelles. Post-transfection, baculovirus particles are amplified through rounds of repeated infections.

D. Cell Culture

Spodoptera frugiperda (Sf-9) cells were purchased in freezer stocks from Invitrogen (Cat. no. 11496-015) thawed, and grown in T-25 flasks in serum free media (Maiorella, 1988). Cells were split and transferred to suspension cultures, kept at 27° Celsius. Cells were maintained in suspension culture at concentrations of 1.0×10^6 cells per mL to 4.0×10^6 cells per mL at 95 percent viability or higher.

Trichoplusia ni (Tn-5) cells were purchased in freezer stocks from Invitrogen (Cat. no. B855-02) thawed, and grown in T-25 flasks in serum free media (Maiorella 1988). Cells were split and transferred to suspension

cultures, kept at 27° Celsius. Cells were maintained in suspension culture at concentrations of 5.0×10^5 cells per mL to 3.0×10^6 cells per mL at 90 percent viability or higher.

E. Viral Amplification

Viral amplification was conducted through controlled Sf-9 infections conducted over spans of two to four days. High viability (greater than or equal to 95% viability) Sf-9 cells at 1.0×10^6 cells per mL density were centrifuged into a pellet at 3,000 rpm using a Damon Division clinical centrifuge Model No. 04507. Supernatant was removed and replaced with inoculum. Cells were incubated with inoculum, rocking for one hour at room temperature. Post-inoculation, cells were sampled in using a Cedex cell sorter to measure viability, density, and diameter. Cells were sampled in the Cedex every day post-infection. A flask of healthy, uninfected Sf-9 cells with identical initial viability and density was used as a control. Post-infection, cultures were centrifuged at 3,000 rpm and supernatant was harvested and filtered, becoming the next inoculum.

F. Protein Expression

Inoculum strength was tested in Tn-5 cells through 72 hour infections. Much like Sf-9 viral amplification infections, Tn-5 protein expression infections contain many similar steps, with some alterations due to differences in species-specific cell growth and protein production capabilities. High viability (greater than or equal to 90% viability) Tn-5

cells at a density of 0.5×10^6 cells per mL were centrifuged into a pellet at 3,000 rpm. Supernatant was removed and replaced with inoculum. Cells were incubated with inoculum rocking for one hour at room temperature. Post-inoculation, cells were sampled in using a Cedex cell sorter to measure viability, density, and diameter. Post-infection, cultures were centrifuged at 3000 rpm and supernatant was harvested for Western blotting and protein purification.

G. Cedex Data Collection

Cell density, viability, and diameter were collected using a Cedex Counting System by Innovatis (Version 1.61, Build 1.61.1604).

Measurements were collected at 24-hour time intervals throughout the duration of Sf-9 and Tn-5 infections.

H. Western Blotting

Supernatant derived from Sf-9 and Tn-5 infections with NEU1 viral stock was stored at 4° C. For Western Blotting, 10 μ L supernatant samples were mixed with 2 μ L 6x SDS Sample Buffer (7 mL 0.5 M Tris pH 6.8, 3 mL glycerol, 1g SDS, 1.2 mg bromophenol blue, ddH₂O to 10 mL) , and the mixture was boiled for ten minutes. Samples were subsequently loaded in a 10% SDS gel and electrophoresed for 1 hour at 165 Volts. Samples were then transferred to a nitrocellulose membrane and probed with anti-Neuraminidase primary antibody (Abnova, cat no. NBP1-00941) at a

concentration of 1:1000, and then probed with AP-conjugated goat anti-rabbit secondary (Pierce cat no. 31340). Treated with BCIP/NBT Color Development Substrate (5-bromo-4-chloro-3-indolyl-phosphate/nitro blue by Promega. Images were captured using InGenius Bio Gel Documentation Imager by Syngene.

I. Small Polyclonal Cell Lines

One technique pioneered extensively by the Garman lab has been the use of small polyclonal and monoclonal Tn5 cell lines. For the selection of the PPCA protein producing cells that produced the most protein we took the contents of one 5 mL T-flask post blastocidin selection and added 100 μ L of suspended cells to each well of a 96-well plate.

While this allowed for a fair amount of selection, there were one to five thousand cells in each well of the 96-well plate. For the NEU1 monoclonal lines, we resuspended and diluted the contents of each 5 mL T-flask (post blastocidin selection) to 100 mL. With these cell suspensions, we created two 96-well plates for each: a 1:1 dilution of cells/media (small polyclonal), and a 1:9 dilution of cells/media (monoclonal).

These plates were allowed to grow for 4 days, and then dot blotted to determine which wells were producing the most protein. The top twelve protein producing wells were resuspended and divided evenly over eight

new wells in a different 96-well plate. Eventually, these cells were grown into increasingly larger cultures.

J. DisEMBL Protein folding and Disorder Prediction

Protein folding and relative ease of crystallization was calculated using the freeware program, DisEMBL (Iakoucheva and Dunker, 2003; Linding et al., 2003). DisEMBL characterizes three different parameters key to proper protein folding: loops and coils, highly mobile loops known as hot loops, and missing coordinates that suggest disorder (Linding et al., 2003). By entering the amino acid sequence of each protein into DisEMBL, one can generate an educated guess about the protein's folding.

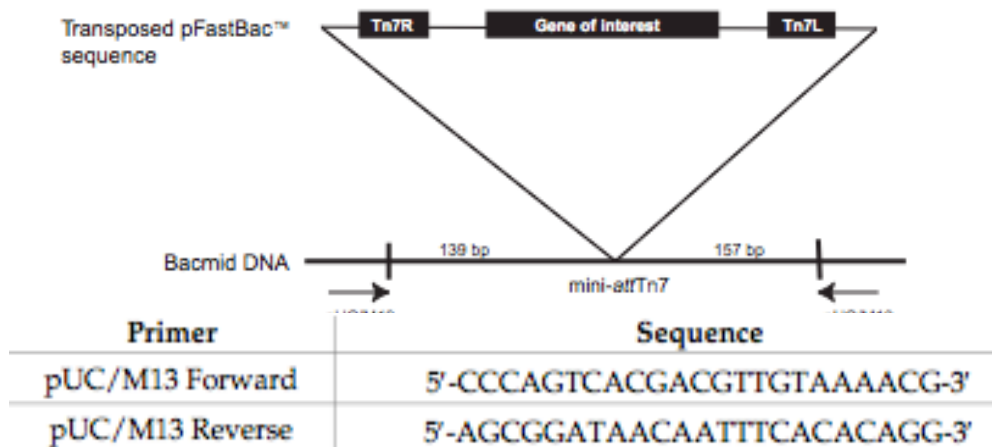


Figure 16 – The design of a bacmid leading to recombinant baculovirus.

The gene of interest is flanked on both sides by identical promoters, and

then inserted into a baculovirus, with 139 base pairs (bp) on one side and 157 bp on the other. The length of the gene must be such that it will fit within the vector (Invitrogen Corporation, 2008).

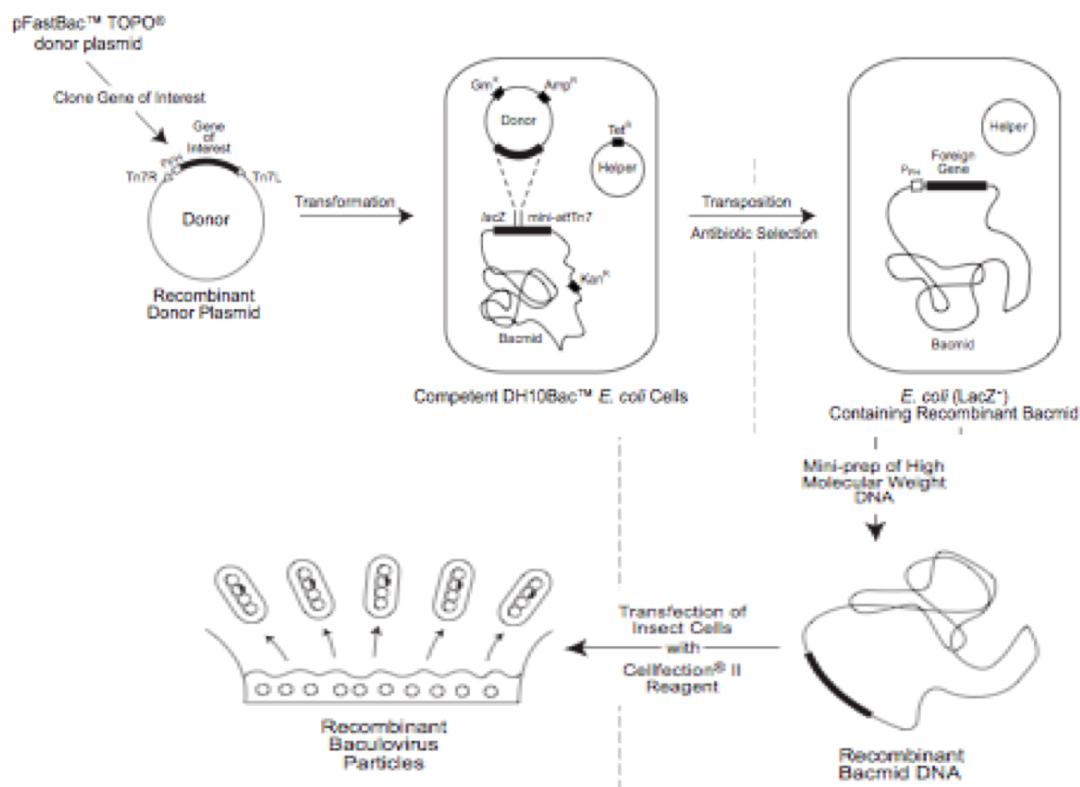


Figure 17 – A method for developing a recombinant baculovirus for protein expression. The gene encoding the protein of interest is inserted into a donor plasmid, which is in turn transformed into *E. coli* cells and transposed into a bacmid. Plasmid DNA extraction yields large quantities of bacmid DNA containing the gene of interest. This DNA is easily transfected into insect cells. Post-transfection, baculovirus particles are

amplified through rounds of repeated infections. (Invitrogen Corporation, 2008).

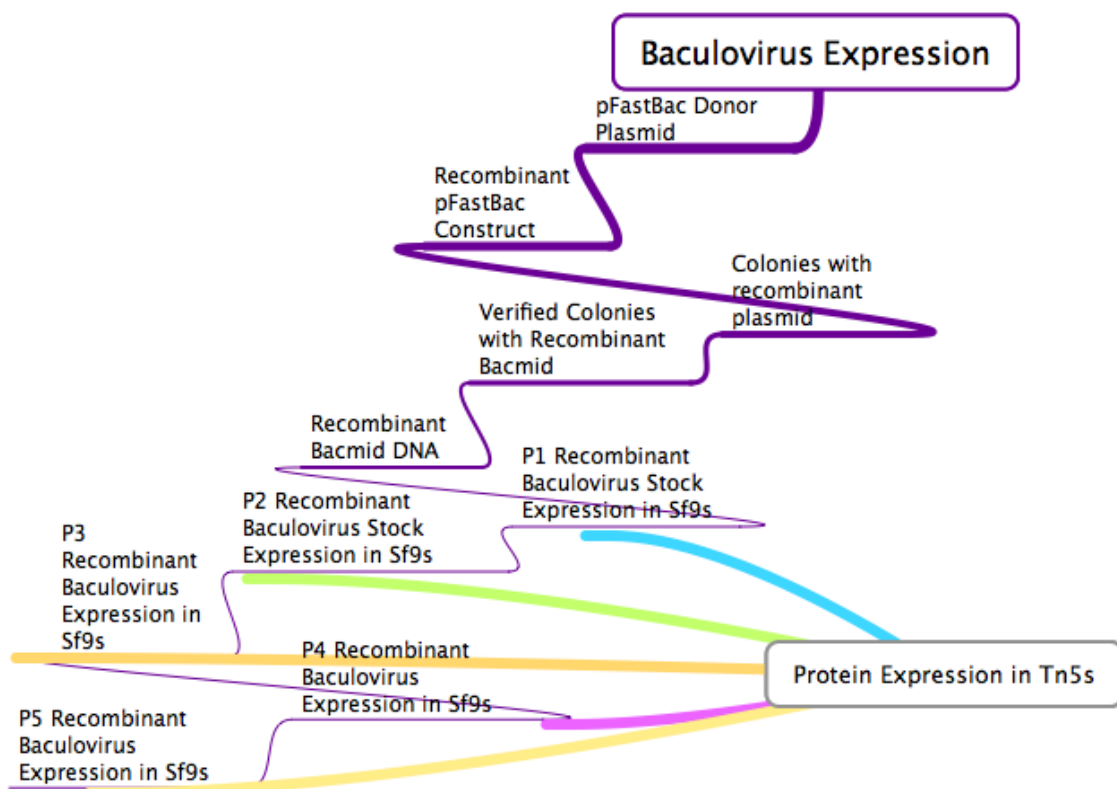


Figure 18 – A chart of the process of baculovirus protein expression from DNA sequence of interest to final high titer viral stock. The first step (starting with a donor plasmid) to obtaining large quantities of recombinant bacmid DNA is performed in an *E. coli* system, while viral amplification takes place in *Spodoptera frugiperda* (Sf-9) cells.

Each colored line points to a separate protein expression experiment.

Signs of Infection	Phenotype	Description
Early (first 24 hours)	Increased cell diameter	A 25–50% increase in cell diameter may be seen.
	Increased size of cell nuclei	Nuclei may appear to "fill" the cells.
Late (24–72 hours)	Cessation of cell growth	Cells appear to stop growing when compared to a cell-only control.
	Granular appearance	Signs of viral budding; vesicular appearance to cells.
	Detachment	Cells release from the plate or flask.
Very Late (>72 hours)	Cell lysis	Cells appear lysed, and show signs of clearing in the monolayer.

Figure 19 – Signs of insect cell infection over the course of a viral amplification, courtesy of Invitrogen. Hallmarks of a standard infection include increases in cell diameter and nuclei, decreases in cell growth, and lysis. These changes in cell size and shape are observed through microscope or Cedex cell sorting (Invitrogen Corporation, 2008).

Results

Chapter 1 – NAGLU Mutagenesis

To generate a construct of NAGLU that contained a C-terminal Strep tag, we performed mutagenesis PCR over a temperature gradient on a NAGLU construct that contained a C-terminal polyhistidine tag. The results of this PCR reaction were electrophoresed on an agarose gel. Figure 20 shows the gel image of this electrophoresis. Using an annealing temperature of 83° C we were able to obtain a band that was the proper size of the pIB.V5-HisTopo vector and the NAGLU gene, 5.7 kb. With these promising results in hand, we gel purified the remainder of the PCR product generated under these conditions.

The results of the gel purification are shown in Figure 21. The purified product was subsequently ligated, introduced into *E. coli*, harvested, and sent for sequencing. The sequences of the DNA did not align with our desired mutagenesis. To determine why sequences did not align, we performed an *Xho* 1 digest, shown in Figure 22. This digest yielded bands at 3 kb and 6 kb, inconsistent with the cut sites for the restriction enzyme. This result indicated that the DNA did not contain the correct vector and insert sequences.

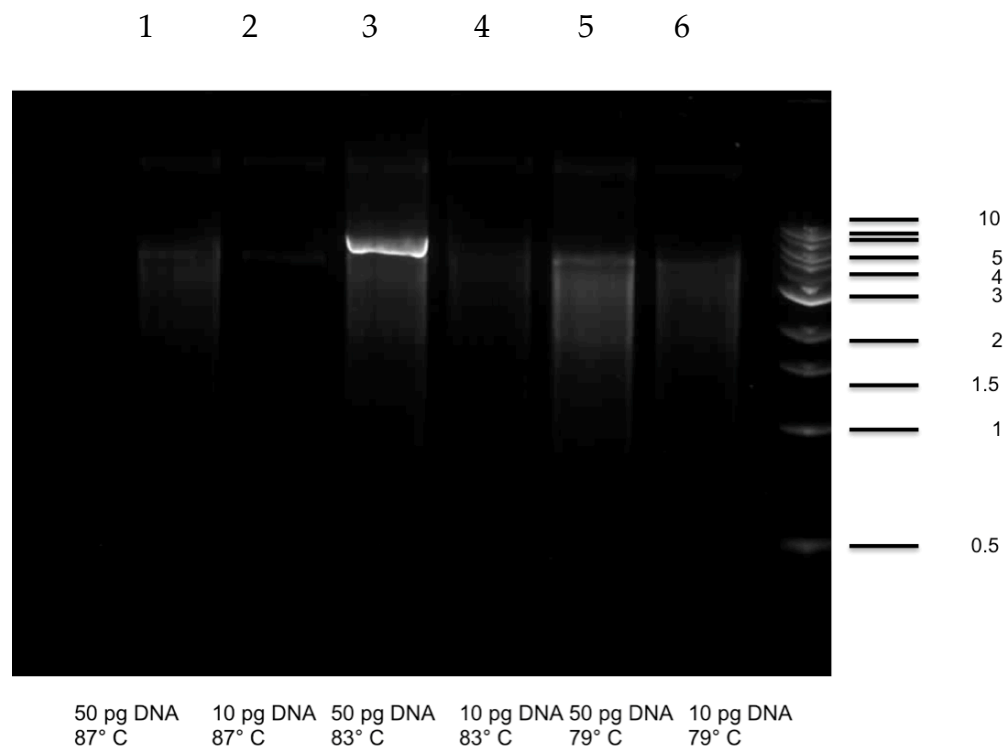


Figure 20. Gel Image showing PCR amplification of the gene of interest over a temperature gradient. NAGLU (2.2 kb) and the pIB.V5-HisTopo vector (3.5 kb) make a total size of 5.7 kb. As shown in lane three, a concentration of 50 picograms DNA and a PCR extension temperature of 83° C contains the appropriate band.

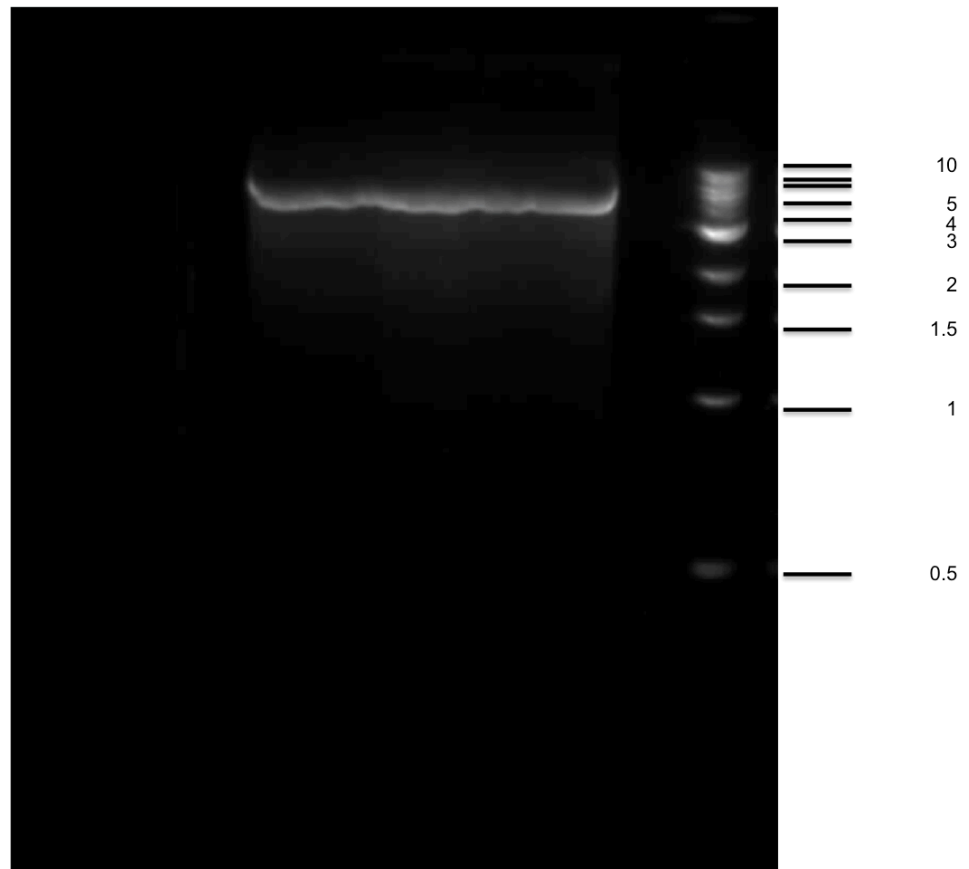


Figure 21. Gel Image of the gel electrophoresis purification of the NAGLU gene and vector PCR product. Together, these yield a size of 5.7 kb.

Curvature at the ends of the band is a result of high DNA concentration.

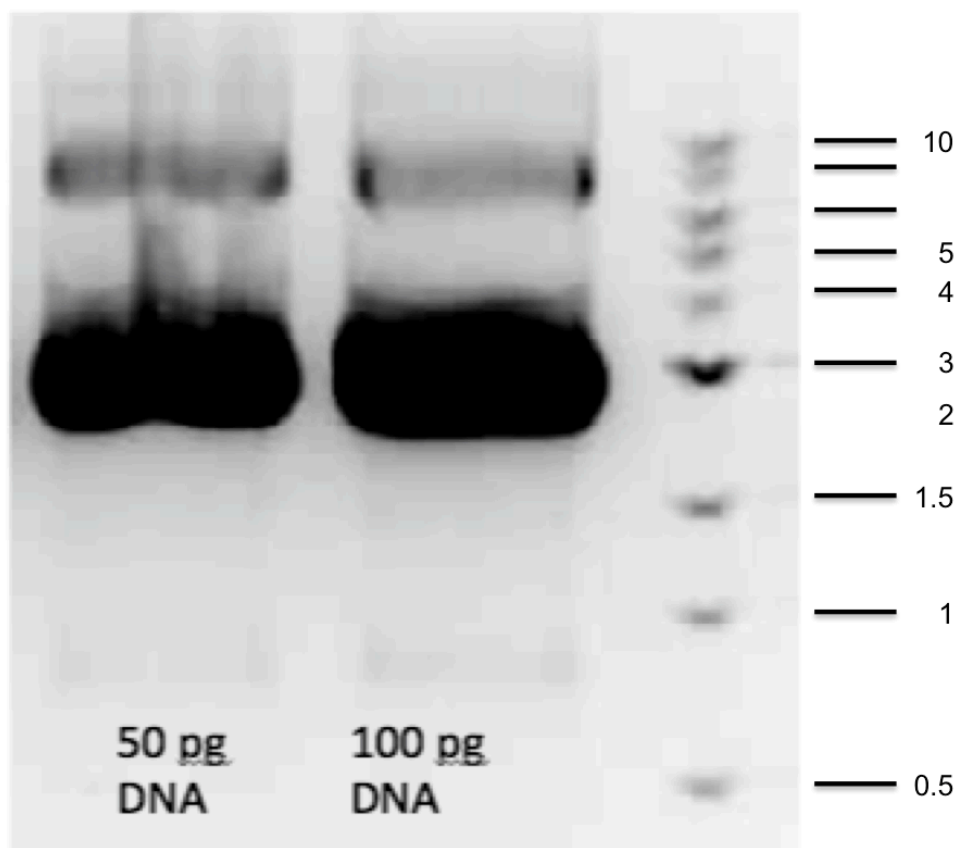


Figure 22. Gel Image of the *Xho* 1 digestion products of the putative PCR amplified NAGLU and vector. There are two distinct bands – one running at about 3 kb and the other at about 6.5 kb. The 6.5 kb is larger than the expected size of insert and plasmid, which should be roughly $2.23+3.5=5.73$ kb. These data suggest that PCR amplification may not have necessarily amplified the gene and vector combination.

I then performed PCR on the NAGLU gene using a mix of sequencing and mutagenesis primers to determine whether the mutagenesis primers were priming appropriately. Sequencing primers were paired with mutagenesis primers. Since both primers should lead to sequences of similar overall length, testing primers in this manner is an efficient way of determining if they have the correct sequence. Figure 23 shows an illustration of the priming of both sequencing and mutagenesis primers.

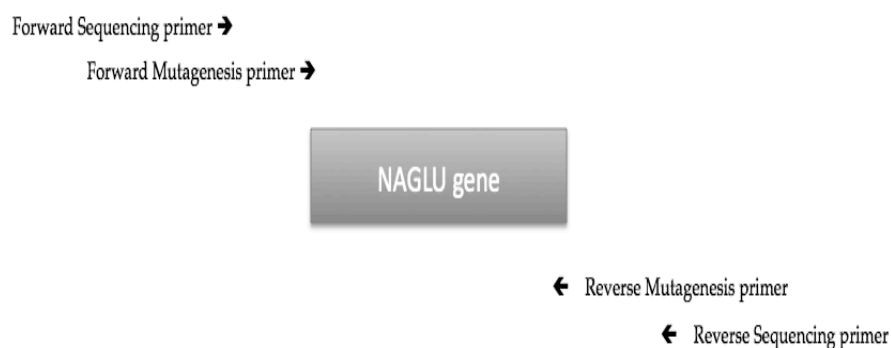


Figure 23. This diagram represents NAGLU primers and their respective regions of priming. To test the NAGLU mutagenesis primers, sequencing primers were paired with mutagenesis primers. Since both primers should lead to sequences of similar overall length, testing primers in this manner is an efficient way of determining if they have the correct sequence.

Figure 24 shows the results of the mutagenesis primer test. The only change introduced by the mutagenesis primers is the addition of the seven

amino acid streptavidin tag. Thus, one would expect to see products only at 5.7 kb. However, only very light bands appear at this size in the RmutFseq lanes. Thus, it is unlikely that the mutagenesis primers are amplifying the NAGLU gene and vector as expected. The forward mutagenesis primer is likely incorrect as no bands of the correct size appear in the RseqFmut lanes, and the reverse mutagenesis primer may be incorrect as well, as indicated by the two bands in the RmutFseq lanes.

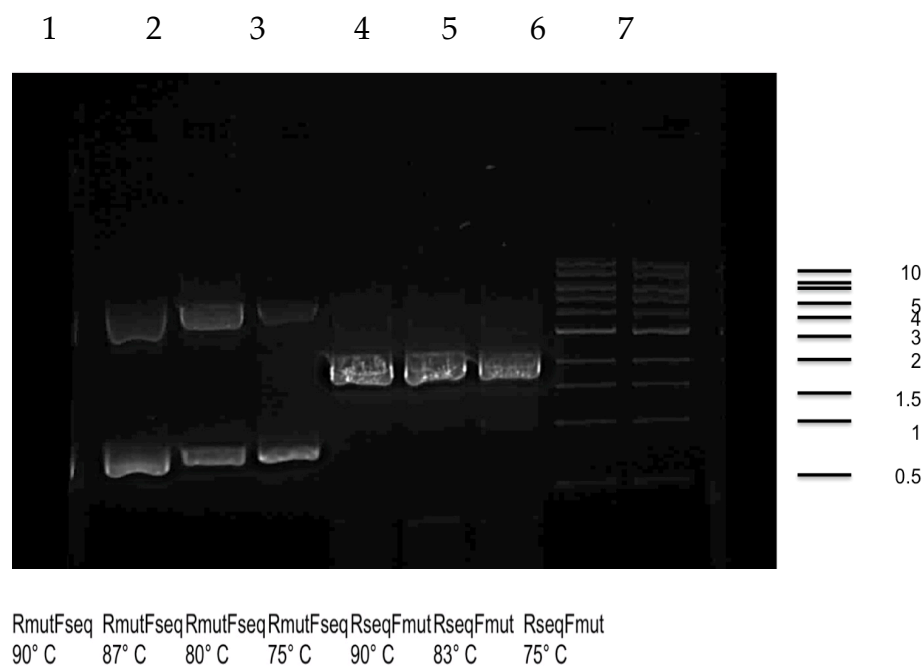


Figure 24. Gel Image of the PCR products of a test of the mutagenesis primers used to amplify the NAGLU gene and vector. RmutFseq indicates a reverse mutagenesis primer with a forward sequencing primer, which has been previously tested. RseqFmut refers to use of a reverse sequencing primer with a forward mutagenesis primer.

Chapter 2 – PPCA Mutagenesis and Stable Cell Line

A construct containing three key mutations was generated. The results of the mutagenesis PCR are shown in Figure 25. Correct mutagenesis was confirmed through DNA sequencing. Plasmids containing NEU1 and PPCA were introduced into Tn5 cells. Supernatant protein was assessed using Western blot analysis, as shown in Figure 26 and Figure 27, which both contain bands indicating the successful incorporation of plasmids containing the NEU1 and the PPCA genes.

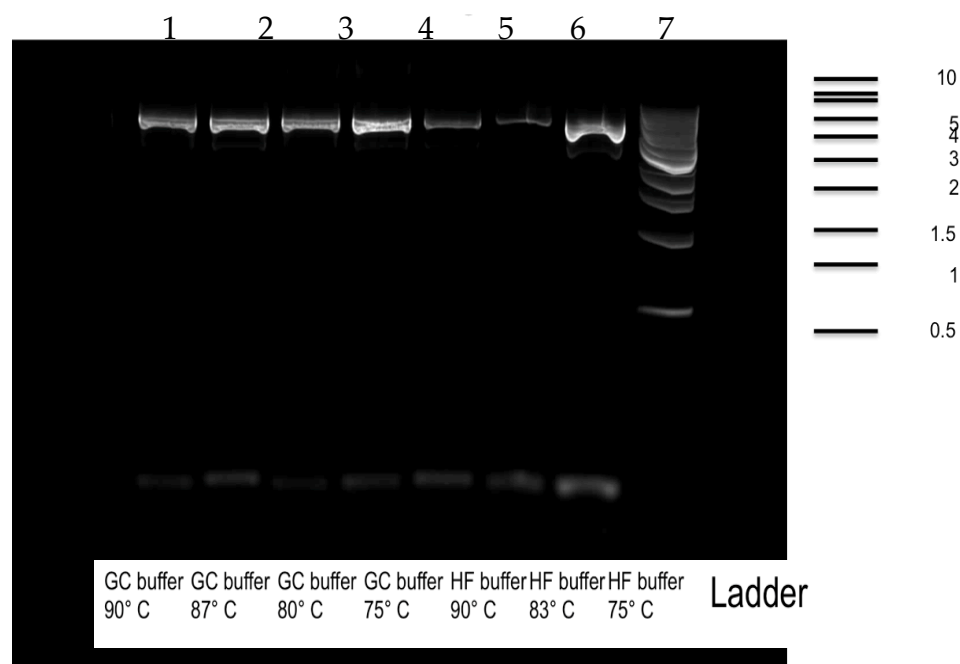


Figure 25. Gel Image of the PCR amplification of the PPCA R284A mutation over a temperature gradient. The band appears at the correct size of 5.4 kb, the length of the gene. This gene encodes the immature PPCA precursor containing its excision peptide. The R284A mutation is designed to prevent PPCA's autocatalytic activity that removes this excision peptide.

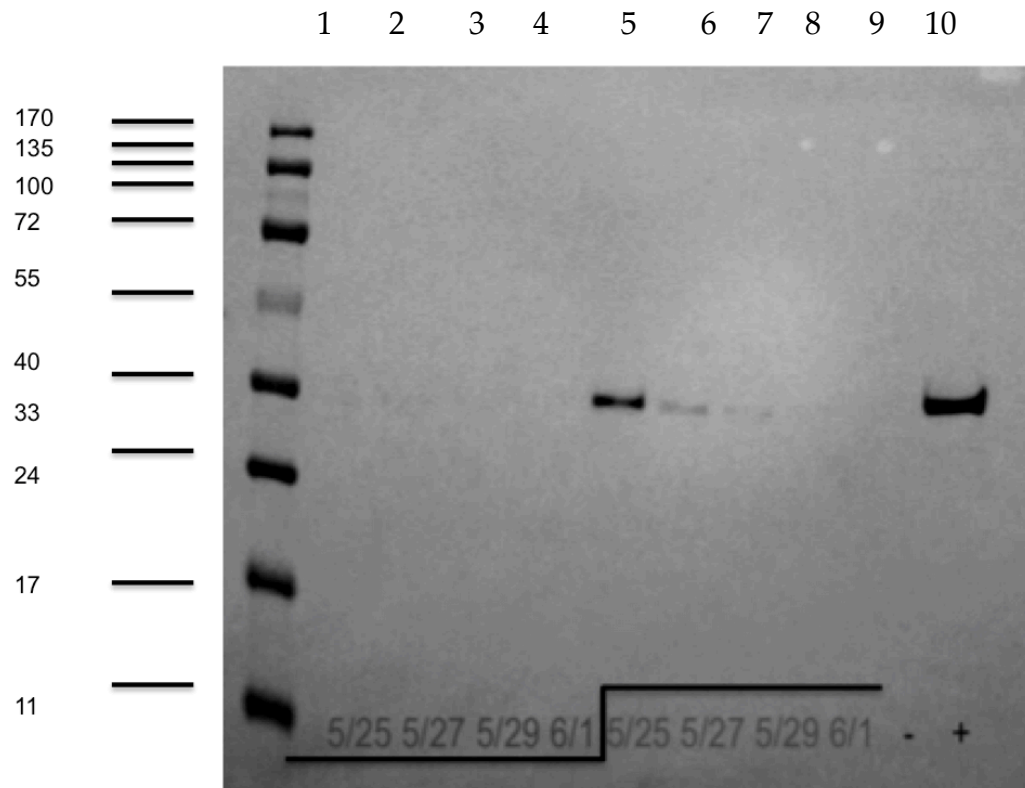


Figure 26. Western blot probed with anti-histidine antibody tested against of supernatant derived from the introduction of PPCA triple mutant plasmids into Tn5 cells. Time points were taken at two to three day intervals. Lanes 2-5 on the left show little to no protein expression, indicating poor uptake of the plasmid. Lanes 6-9 show a gradual decrease in protein production over time corresponding directly to blastocidin cell stress during the selection process.

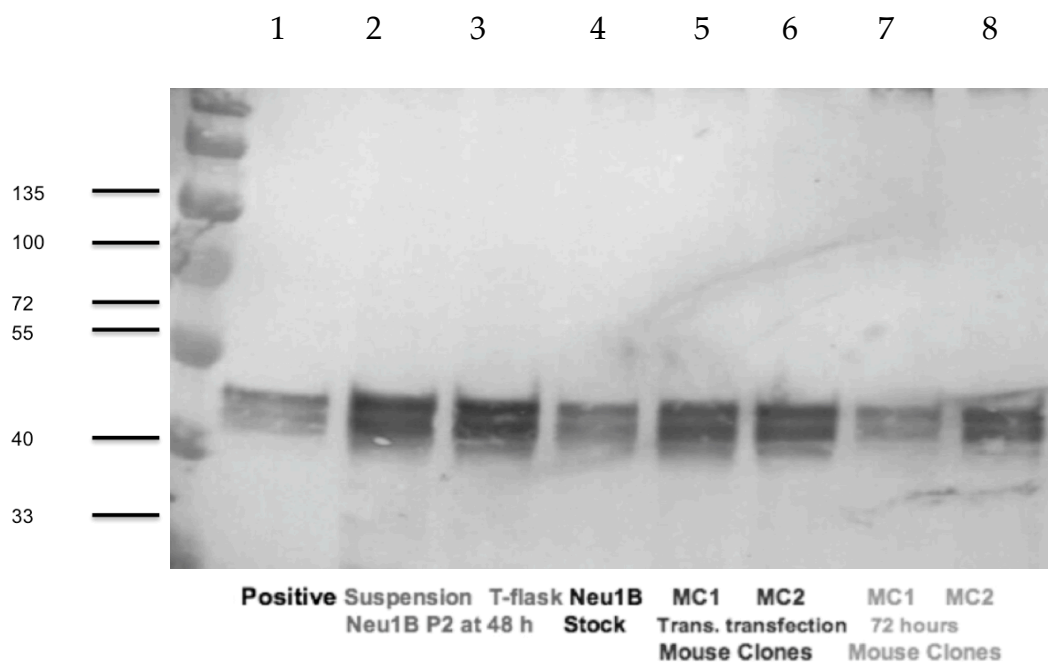


Figure 27. Western blot of baculovirus transfection probed with Anti-Neu1 antibody.

Small polyclonal NEU1 and PPCA stable cell lines were also generated. Figures 28 and 29 show immunodot blots derived from the supernatant of each well of the 96-well plates containing small polyclonal lines.

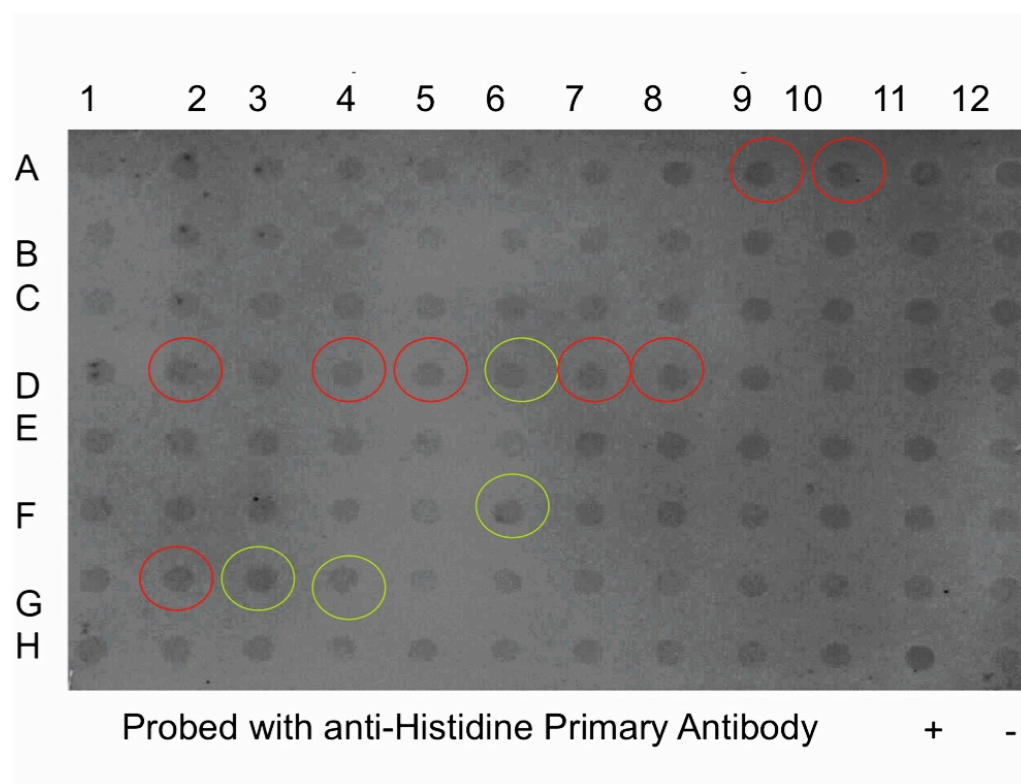
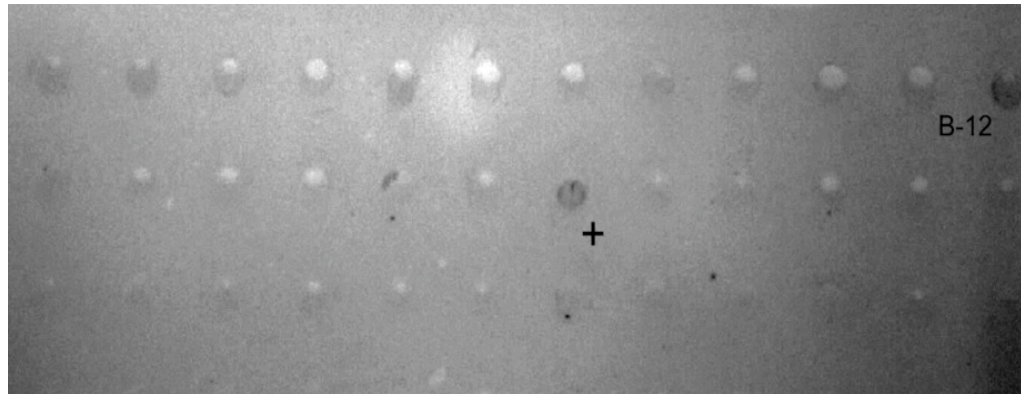


Figure 28. Immunodot blot showing protein production of PPCA triple mutants probed with anti-histidine antibody. Wells circled in red appear the darkest, and thus have higher protein expression, followed by the wells circled in green, which have the next highest protein expression. Cells from circled wells were subsequently passaged and maintained. Measurements are normalized to the darkness of the negative control (H12).

A



B

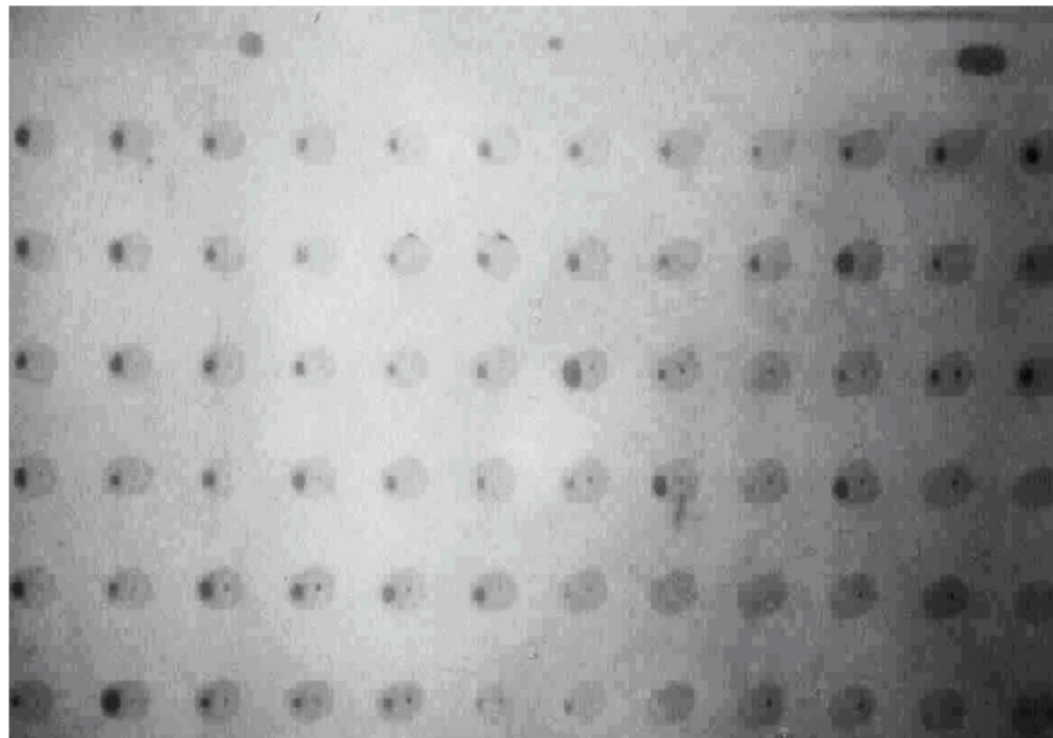


Figure 29. A. An immunodot blot of protein produced for the PPCA triple mutant, probed with an anti-histidine antibody. B. Immunodot blot of protein generated by the human NEU1 stable cell line. The blot is probed with Anti-NEU1 antibody.

Chapter 3 – Viral Amplification of Neu1

Two-year-old NEU1 viral stocks were assessed for infection strength in Tn-5 protein producing cells (Figures 30, 31, and 32). Tn-5 cells were incubated with various volumes of inoculum and media for a period of 72 hours, at which point media was harvested for Western Blot analysis. Results, shown in Figure 34, indicate that while initial viral stocks generated in Sf-9 cells no longer contain protein, infection in Tn-5s allows for the production of a moderate amount of NEU1 protein.

After confirming that the inoculum had a high enough titer to warrant further amplification, five rounds of viral amplification were performed in Sf-9 cells. Initial volume of inoculum for P1 generation was 12.5 mL. Throughout the course of Sf-9 amplification, volume of inoculum was decreased to 2 mL, and volume of infection was increased from 15 mL to 30 mL. Each infection was carried out over a period of 48 to 96 hours. Supernatant collected at the end of each infection became inoculum for the next generation of virus.

Once five rounds of amplification in Sf-9 cells had been performed, 2 mL of each generation of Sf-9 cell amplification were used as inoculum for a 30 mL flask of Tn-5 cells. The results of these Tn-5 infections are shown side by side with their corresponding inoculum stocks in Figure 34, a Western blot of supernatant derived from each infection at termination.

After determining that very little P5 inoculum is necessary for significant protein production, I can scale up protein production for purification.

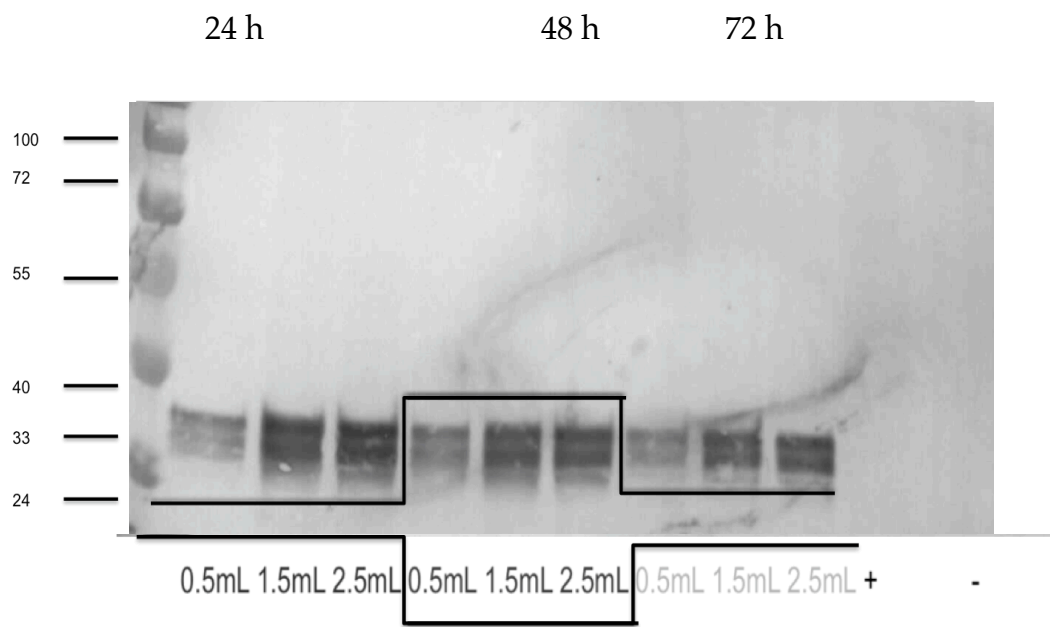


Figure 30. Western Blot of viral Tn5 infection supernatant probed with Anti-Neu1 Primary Antibody showing the expression of protein over a 72-hour time course. 1st 3 are 24 h, 2nd 3 are 48h, 3rd 3 are 72 h.

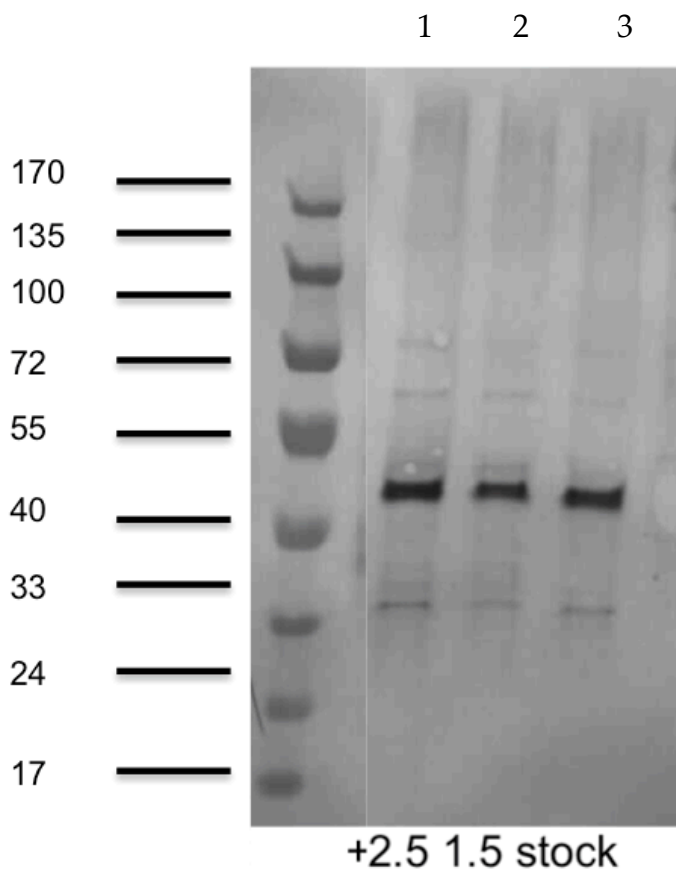


Figure 31. Western blot of human Neu1 viral expression in two-year-old inoculum probed with anti-histidine antibody.

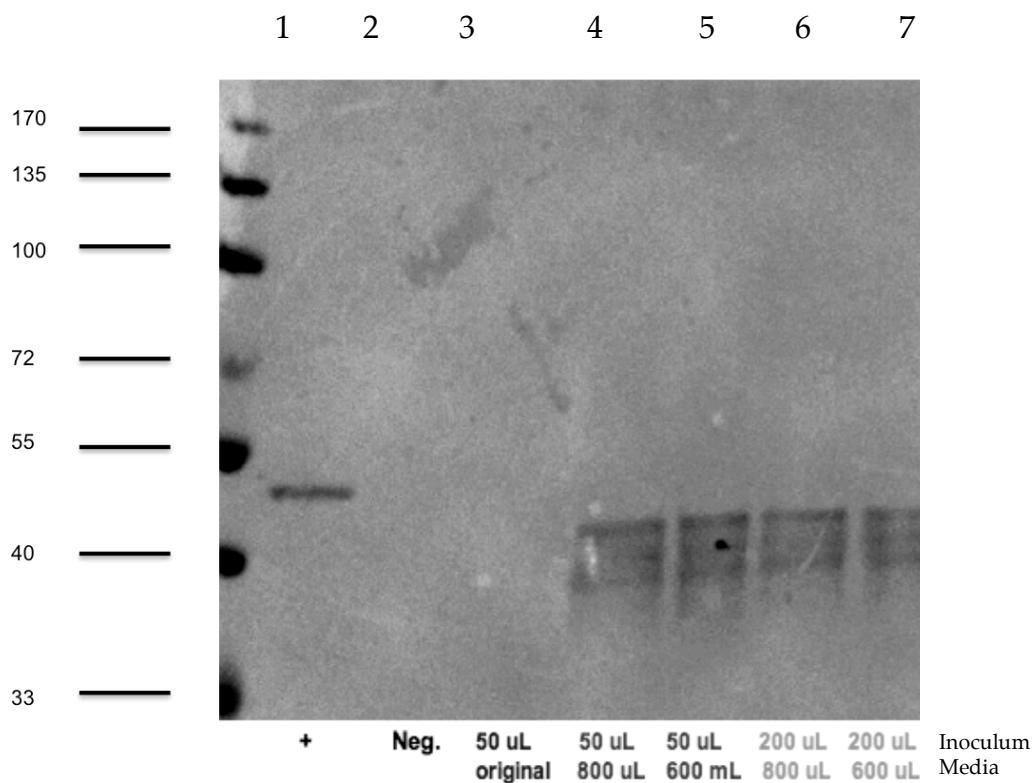


Figure 32. Western blot of viral infection probed with anti-Neu1 antibody. Infection of Tn-5 cells with various amounts of inoculum and media. The top number in each lane represents the volume of inoculum used, while the bottom number indicates the volume of media used. 50 uL original indicates that pure inoculum was run in lane 3.

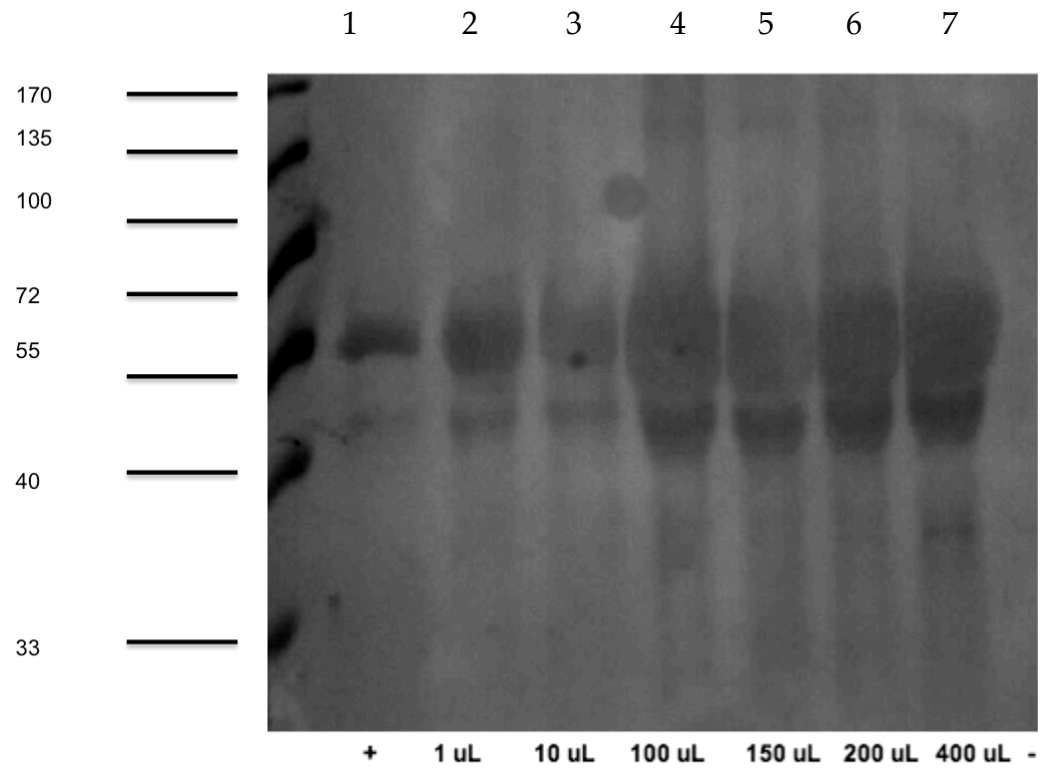


Figure 33. Western blot of protein supernatant harvested from a NEU1 sample infection probed with Anti-NEU1 primary antibody.

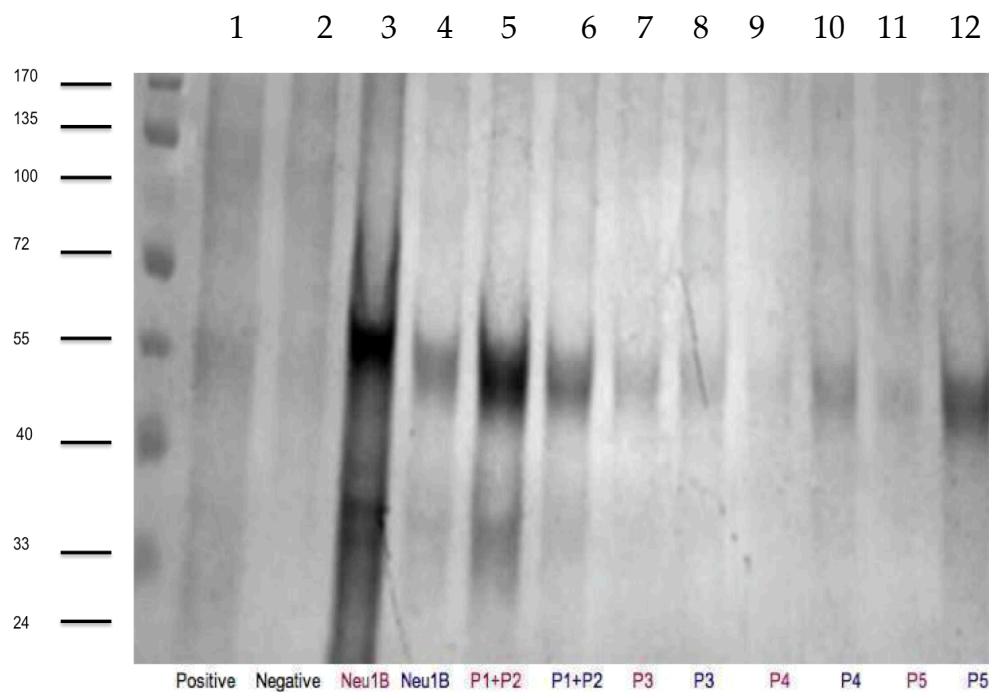


Figure 34. Western blot probed with anti-Neu1 antibody. This blot shows five generations of Sf-9 cell amplification (shown in pink above) next to the Tn-5 cells they infected. Neu1B represents the original viral stock from which amplifications began. The results of these infections indicate that viral titer has been increasing while protein present in the inoculum has been decreasing. Strong bands for Sf-9 inoculum in Neu1B, P1+P2, and P3 represent large amounts of protein present in stock, but not necessarily a high viral titer. Increasingly large bands in Tn-5 infections indicate a corresponding increase in Sf-9 amplification viral titer, and therefore a strengthening in viral stock. To optimize protein expression further, using the strongest P-5 Sf-9 amplification derived viral stock; Tn-5 cells were infected at volumes of inoculum. The numbers of viable cells per mL and

cell diameter were measured every 24 hours over the course of the 72-hour infection, and are shown in Figure 3 and Figure 4.

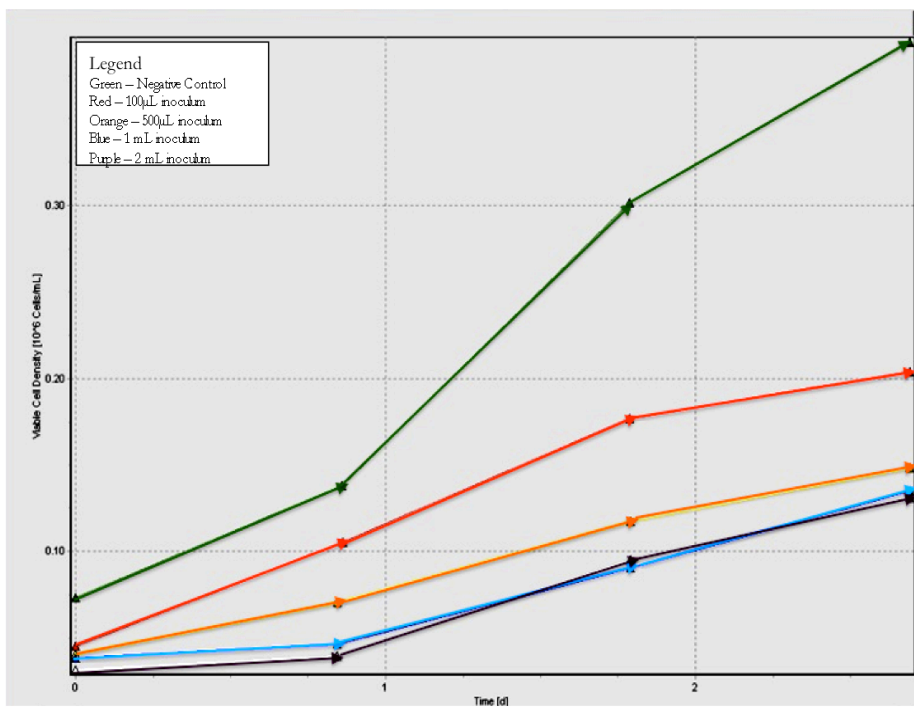


Figure 35. Graph representing the viable cell density of each Tn-5 cell infection over the course of 72 hours. As expected, the green line (negative control) shows the highest viable cell density by 72 hours and the purple line (2 mL inoculum) shows the lowest viable cell density after 72 hours.

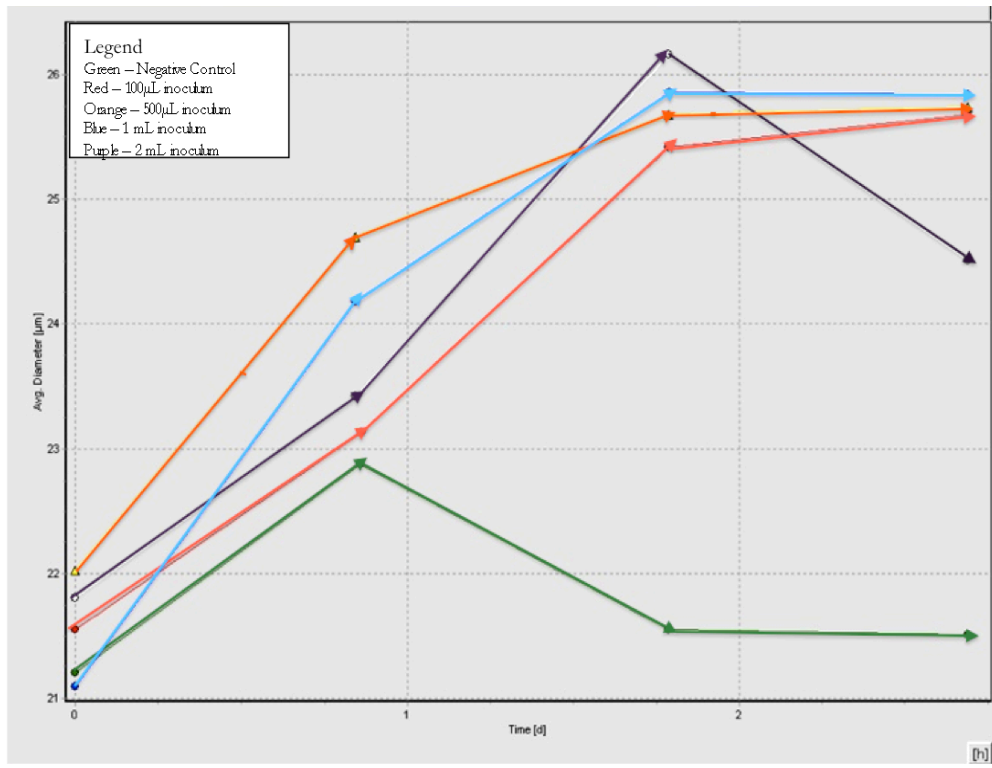


Figure 36. Graph representing the cell diameter in microns of each Tn-5 cell infection over the course of 72 hours. As expected, the green line (negative control) shows the lowest diameter (less than 22 microns) by 72 hours. Infection as tracked by diameter appears to peak at 48 hours for the 2 mL inoculum culture, but peaks at 72 hours for the other cultures containing lower volumes of inoculum.

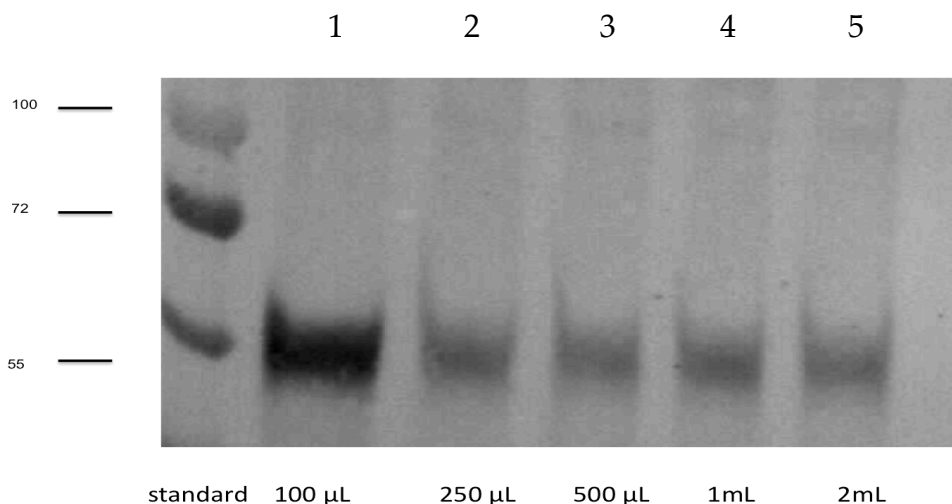


Figure 37. Western blot of harvested supernatant from a Neu1 infection of Tn5 cells probed with an anti-Neu1 antibody. These data indicate that 100 μ L is the best inoculum volume for a 30 mL infection.

Protein produced through this infection of Tn-5 cells was visualized through Western blotting. Interestingly, the 100- μ L culture of Tn-5 cells resulted in the greatest protein generation. This finding may be a result of secondary infections generated with the lower amount of inoculum. It is possible that higher volumes of inoculum yield a higher initial volume of protein through the 48-hour time point, but do not lead to a large number of secondary infections which may take place more readily when lower amounts of cells become initially infected, which then pass on their infection to other cells, ultimately leading to higher protein production.

Protein disorder calculations were generated using the open source software DisEMBL. DisEMBL is a program that assesses the predicted

disorder of a protein using three different metrics: loop-coil, “Remark,” which refers to areas that are usually disordered in crystal structures, and hot loops, which are often disordered, as well. Falling under the disorder probability of 0.5 or less indicates that it is likely that a protein will be ordered enough to crystallize. Figures 38, 39, and 40 which represent the predicted disorder for NAGLU, NEU1 and PPCA respectively contain disorder that falls within these bounds. Thus, it is likely that these proteins will crystalize.

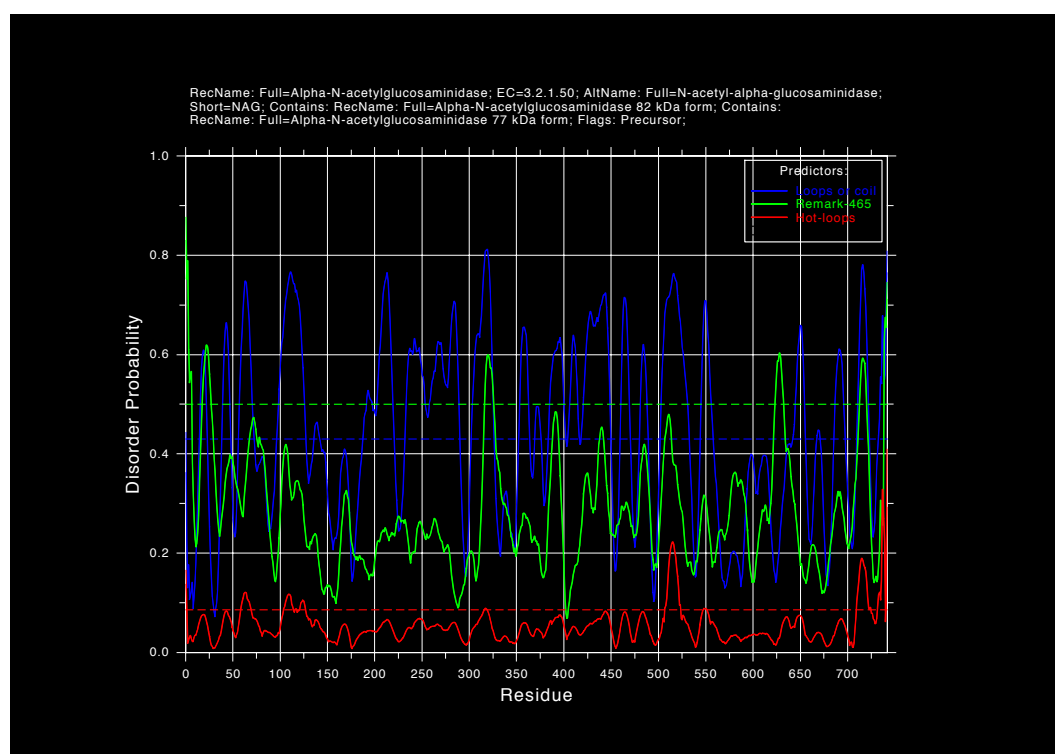


Figure 38. A graph representing the disorder probability in human NAGLU generated using the program DisEMBL.

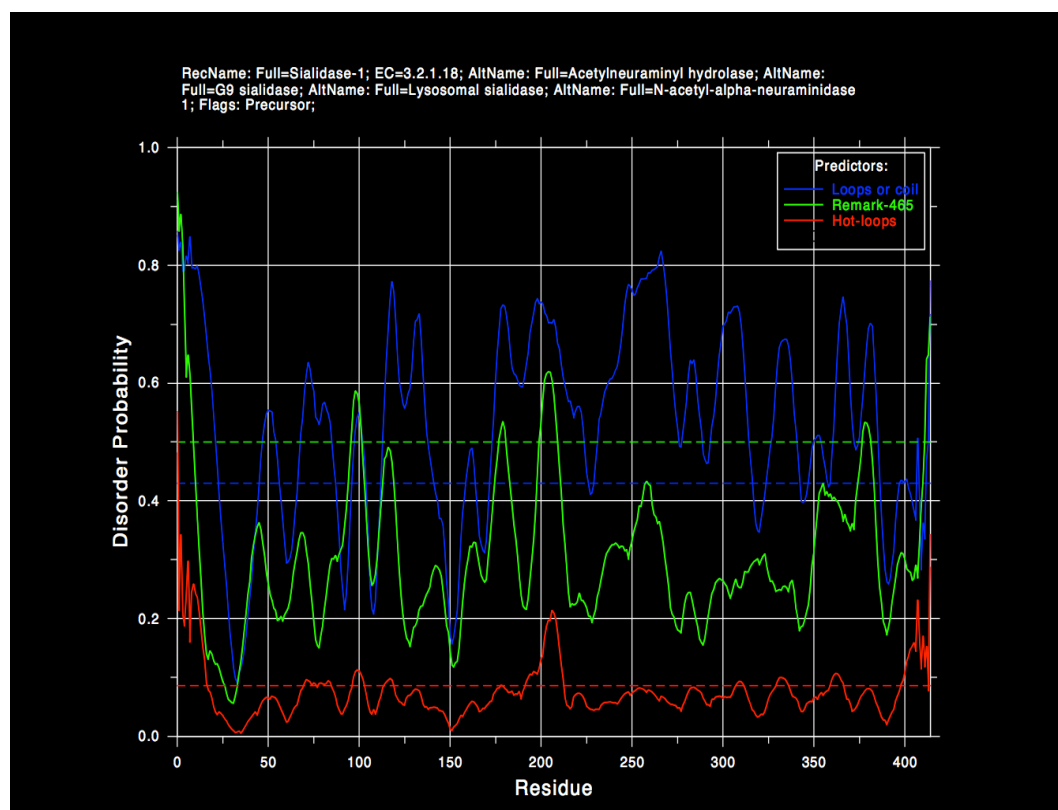


Figure 39. A graph representing the disorder probability in human NEU1 generated using the program DisEMBL. This program allows the user to determine how likely it is that a given protein will successfully from a crystal lattice suitable for x-ray crystallography.

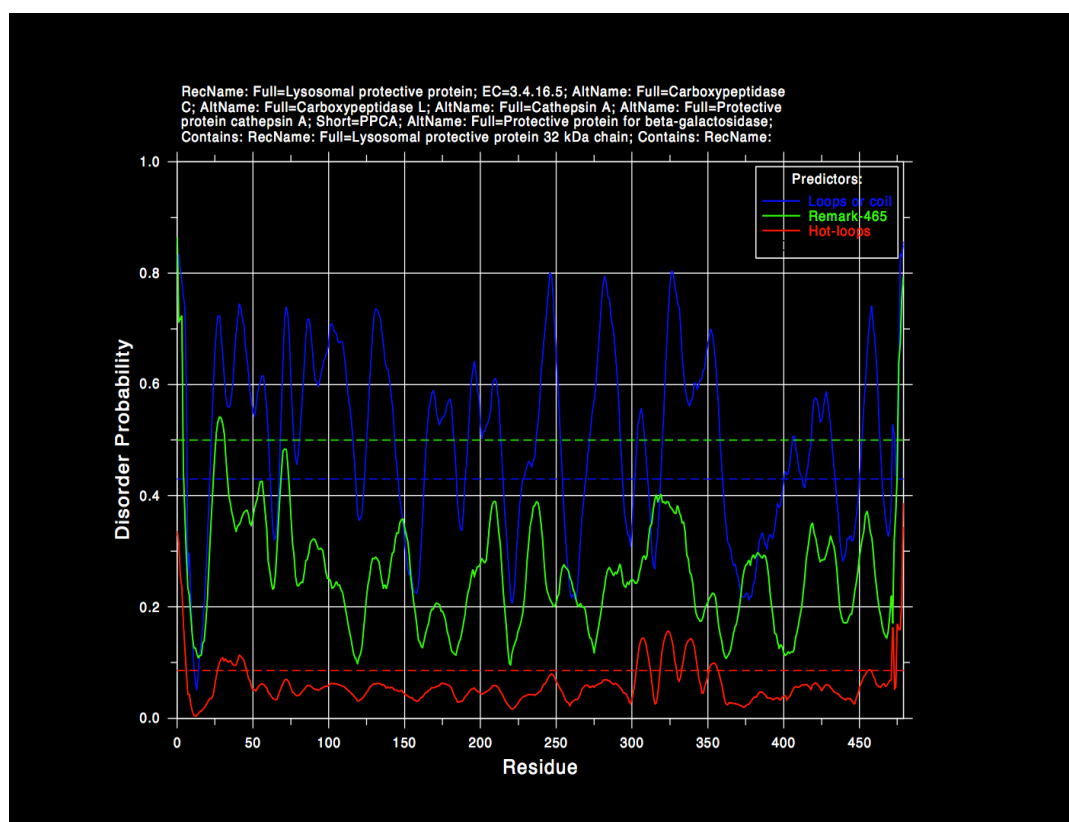


Figure 40. A graph representing the disorder probability in human PPCA generated using the program DisEMBL.

Discussion

Mutagenesis

It is likely that the NAGLU mutagenesis discussed in Chapter 1 did not yield the correct sequences due to improper primer sequences. Figure 23 demonstrates the improper priming performed by NAGLU mutagenesis primers. The forward mutagenesis primer does not appear to prime properly, as none of the bands featuring this primer appear at the correct size.

The ligation was repeated multiple times because successful ligation did not seem to occur. Five, ten, fifteen and twenty-minute ligations were attempted, and an overnight ligation, which yielded colonies. DNA concentration was low and did not seem robust, either. When plasmid DNA extraction was successful, DNA concentrations fell mostly between 0.1 ng/ μ L and 30 ng/ μ L. When colonies were sent for sequencing, sequences did not align. In hindsight, ligation, concentration, and sequencing problems were likely related to improper priming.

Unlike the problematic NAGLU mutagenesis, PPCA triple mutant mutagenesis was successful throughout. PCR products appeared at the correct sizes when electrophoresed and contained the proper mutations when the vector and mutant *CSTA* gene were

sequenced. Successes in the cloning of PPCA likely result from appropriate DNA concentrations during mutagenesis PCR and from proper ampicillin selection.

Stable Cell Line Generation

Introduction of plasmids into *Trichoplusia ni* cells and selection through blastocidin has proved an effective means of protein production. Western blots, derived from the supernatant of transient transfections, as shown in Figure 26 and Figure 27, confirm that protein production is successfully taking place in both the cases of PPCA and NEU1 stable cell lines. While blastocidin selection of cells does reduce protein production temporarily during the selection process, it is suspected that most production capabilities will be regained after selection is completed. Successes in stable cell line generation of PPCA and NEU1 have allowed for the generation of cultures large enough to generate protein crystals.

Monoclonal and Small Polyclonal Stable Cell Line Generation

In an effort to increase quantity of protein production over time, we have generated monoclonal and small polyclonal stable cell lines. Figure 28 and Figure 29 show the immunodot blots generated from protein supernatant assays collected from very small numbers

of cell colonies grown in 96-well plates. On the whole, monoclonal and small polyclonal cell lines seem an effective way to boost protein production, at least on a very small scale, though I have not yet confirmed these results through large-scale cultures.

Figure 29A provides a powerful example of the difference in protein production across wells. Well B-12, for instance, has much greater protein production than all other wells on the plate, save the positive control. Figure 29B, on the other hand, demonstrates the weaknesses of the immunodot blot assay method. It is very hard to definitively determine the well with the greatest protein production, however it is clear that some wells contain more protein than others, and that some wells can be eliminated purely on the grounds of low protein production.

Thus, while immunodot blots are high in qualitative information about protein production, they are low in quantitative data. With mutations targeted at the PPCA active site, it would be impossible to perform activity assays on supernatant, and Western blotting is not a viable option considering the large number of wells under consideration. As such, the immunodot blot is the best means at present for understanding protein expression, though it is imperfect.

NEU1 Baculovirus work

Amplification of two-year-old NEU1 baculovirus stocks has allowed me to learn a great deal about the preservation of titer and means of strengthening a viral stock. A key lesson gained from a thorough exploration of viral amplification has led me to better understand the infection process.

Figures 30 through 32 are the products of my attempts at attaining a qualitative examination of viral strength and necessary inoculum volume. Unfortunately, the blots generated likely contained protein present mainly in the inoculum added to cells, rather than that generated by infection and subsequent cell lysis. This largely explains the similarity in protein expression across samples. Figure 33 begins to yield information more directly relevant to inoculum volume and protein production, demonstrating that larger volumes of inoculum may, in and of themselves, contain more protein. However, the largest inoculum volumes appear to yield lower secondary infections, and therefore are less successful in generating an optimal infection.

Through multiple rounds of viral amplification in Sf9s and expression in Tn5s shown in Figure 34, I have been able to gain a greater understanding of the infection and amplification process.

Use of DisEMBL, an open source piece of software, has allowed me to examine the probable folding of each protein I have studied. Such predictions allow for the characterization of probable folding

of proteins into a crystal lattice. On the whole, very little disorder is predicted for NAGLU, NEU1, and PPCA based solely on the small number of anticipated highly mobile (hot) loops in the structure (Linding et al., 2003). Thus, DisEMBL calculations suggest, in broad terms, that these proteins should crystallize.

Once expression has successfully been optimized, the next step in the structural determination process is protein purification. Purification through the use of nickel affinity columns (which bind polyhistidine tags on the C terminal ends of the proteins) and sizing columns will allow for the generation of protein pure enough to attempt crystallization, the desired outcome of this work. Many of the questions that have prompted crystallographic explorations of the lysosomal complex of PPCA and NEU1 warrant exploration through means other than crystallography. These questions include: which amino acid residues in the PPCA and NEU1 interface participate in binding? What is the native oligomeric state of NEU1? Is NEU1 more catalytically active in the presence of PPCA because PPCA disrupts NEU1's oligomers, or because a one to one ratio must exist between NEU1 and PPCA for binding to take place?

Crystallography is the first and most obvious method to address these questions, but there are many other means. Use of coimmunoprecipitation would help characterize the NEU1/PPCA complex in greater detail. Immunoprecipitation (IP) assays, also known as pull downs, involve

binding one protein (such as PPCA) to an affinity column, adding antibody, precipitating the antigen, and washing the column (Phizicky and Fields, 1995). Bound proteins elute for analysis. IP assays would help in the determination of PPCA and NEU1 residues that participate in binding.

To pinpoint the specific residues involved in NEU1/PPCA binding, biophysical techniques such as surface plasmon resonance (SPR) and isothermal calorimetry (ITC) would be well employed. To use SPR, PPCA could be bound to a chemical layer, and a biotinylated solution NEU1 could be passed across the surface. The addition of streptavidin (a 53 kDa protein that binds biotin with a very high affinity) would cause the resonance to shift (Harris, 2003). This shift could be measured and used to determine whether the NEU1 proteins binding to PPCA were in oligomeric or monomeric form.

ITC is a method used to thermodynamically characterize the energetic relationships of protein-ligand interactions and also protein-protein interactions (Lopez and Makhatadze, 2002). Through precise titration of one protein (for instance PPCA) into a solution of the other protein and measurement of the change in temperature, it is possible to gain quantitative information about protein binding. Use of ITC would allow us to determine a stoichiometric binding constant for the interaction between PPCA and NEU1.

Once we have obtained ΔH through ITC, we can then obtain the

change in Gibbs free energy associated with the interaction, ΔG , as

$$\Delta G = -RT \ln K_a \quad [1]$$

Having obtained the change in enthalpy of the reaction, it is a straightforward task to determine the change in Gibbs free energy for the binding interaction.

$$\Delta G = \Delta H - T\Delta S \quad [2]$$

Combining equation [1] with the definition of change in Gibbs free energy, equation [2], allows us to write

$$\Delta H = T(\Delta S - R \ln K_a) \quad [3]$$

and thus calculate the equilibrium constant, K_a . With K_a in hand, we can then determine c , the unitless parameter indicating strength of binding, using the equation

$$c = K_a \cdot [P_t]^n \quad [4]$$

in which $[P_t]$ is protein concentration, and n is the stoichiometric coefficient (Lopez and Makhatadze, 2002).

High c values indicate tighter binding, while low c values are characteristic of weaker binding interactions. In general, binding reactions associated with a positive ΔH are the result of the disruption of hydrophobic interactions, while those with a negative ΔH are the result of the formation of more hydrophobic interactions.

Electron microscopy (EM) is another possible method to achieve structural data about the NEU1/PPCA binding interaction. EM is a method for determining proteins down to their fold structure. While not

yet capable of the resolution obtainable via x-ray crystallography, EM is a valuable asset in structural determination. While proteins only a molecule thick are not sufficient for x-ray crystallography, they are possible for EM studies. Thus, if only small amounts of NEU1 and PPCA were achievable in future research, EM might be the ideal technique for structural characterization.

Structural data of NEU1 might also be achieved to a high resolution using high pressure Nuclear Magnetic Resonance (NMR). High pressure NMR coupled with a reverse micelle method is another possible method to achieve a NEU1 structure (Ehrhardt et al., 1999). By confining a protein within a smaller area, the Gibbs free energy of the folded state becomes lower than free energy of the unfolded state, forcing large proteins into their native structures and allowing for more dipole couplings that yield structural information (Valentine et al., 2006).

To better understand whether there is a conformational change that arises from the binding interactions of NEU1, PPCA, and GLB1, Dual polarization interferometry (DPI) could be utilized. DPI is a technique in which laser polarization is rotated to excite different polarization modes of two waveguides (Biosensors & bioelectronics, 2006). These measurements allow for the calculation of a refractive index and the thickness layer adsorption. From these measures, we can come to a better understanding of how NEU1 and PPCA interact with each other in solution.

Small-Angle x-ray scattering (SAXS), like EM, is another biophysical technique used to gain structural information about proteins without obtaining the protein crystals necessary for x-ray crystallography (Bouwstra et al., 1991). SAXS would allow for a rough determination of the oligomeric form of NEU1, and possibly some information about the general shape of the lysosomal complex of NEU1, PPCA, and GLB1.

In conclusion, once protein expression of NEU1 and PPCA has been optimized, there are many avenues for fruitful scientific investigation. While x-ray crystallography is the first method of interest, many other biophysical and biochemical techniques could shed light on the PPCA/NEU1 binding interaction.

REFERENCES

- Badash, M. (2009). Your Health - Fabry Disease. Your Health. Available at: <http://www.aurorahealthcare.org/yourhealth/healthgate/getcontent.asp?URLhealthgate=23863.html>.
- Biosensors & bioelectronics (2006). (Elsevier Applied Science).
- Bishop, D. F., Kornreich, R., and Desnick, R. J. (1988). Structural organization of the human alpha-galactosidase A gene: further evidence for the absence of a 3' untranslated region. *Proc Natl Acad Sci U S A* 85, 3903-7. Available at: http://www.ncbi.nlm.nih.gov/entrez/query.fcgi?cmd=Retrieve&db=PubMed&dopt=Citation&list_uids=2836863.
- Bonten, E., Campos, Y., Zaitsev, V., Nourse, A., Waddell, B., Lewis, W., Taylor, G., and d'Azzo, A. (2009a). Heterodimerization of the Sialidase NEU1 with the Chaperone Protective Protein/Cathepsin A Prevents Its Premature Oligomerization — *JBC*. *JBC*, 28430-28441. Available at: <http://www.jbc.org/content/284/41/28430.abstract> [Accessed November 12, 2010].
- Bonten, E., and d'Azzo, A. (2000). Lysosomal neuraminidase catalytic activation in insect cells is controlled by the protective protein/cathepsin A. *JBC* 10, 37657-37663. Available at: <http://www.jbc.org/content/275/48/37657.abstract> [Accessed November 12, 2010].
- Bonten, E. J., Campos, Y., Zaitsev, V., Nourse, A., Waddell, B., Lewis, W., Taylor, G., and d'Azzo, A. (2009b). Heterodimerization of the Sialidase NEU1 with the Chaperone Protective Protein/Cathepsin A Prevents Its Premature Oligomerization. *Journal of Biological Chemistry* 284, 28430.
- Bouwstra, J. A., Gooris, G. S., van der Spek, J. A., and Bras, W. (1991). Structural Investigations of Human Stratum Corneum by Small-Angle X-Ray Scattering. *J Investig Dermatol* 97, 1005-1012. Available at: <http://dx.doi.org/10.1111/1523-1747.ep12492217> [Accessed April 29, 2011].
- Brady, R. O., and Schiffmann, R. (2000). Clinical features of and recent advances in therapy for Fabry disease. *JAMA: The Journal of the American Medical Association* 284, 2771.

- Brady, R. O. (2006). Emerging strategies for the treatment of hereditary metabolic storage disorders. *Rejuvenation Res* 9, 237-44. Available at: http://www.ncbi.nlm.nih.gov/entrez/query.fcgi?cmd=Retrieve&db=PubMed&dopt=Citation&list_uids=16706651.
- Chung, I., Taticek, R., and Shuler, M. Production of human alkaline phosphatase, a secreted, glycosylated protein, from a baculovirus expression system and the attachment-dependent cell line *Trichoplusia ni* BTI-Tn 5B1-4 using a split-flow, air-lift bioreactor. *Biotechnol. Prog.* 9, 675-678. Available at: <http://pubs.acs.org/doi/abs/10.1021/bp00024a018> [Accessed October 21, 2010].
- Desnick, R. J. (2004). Enzyme replacement therapy for Fabry disease: lessons from two alpha-galactosidase A orphan products and one FDA approval. *Expert opinion on biological therapy* 4, 1167–1176.
- Desnick, R. J., Banikazemi, M., and Wasserstein, M. (2002). Enzyme replacement therapy for Fabry disease, an inherited nephropathy. *Clin Nephrol* 57, 1-8. Available at: http://www.ncbi.nlm.nih.gov/entrez/query.fcgi?cmd=Retrieve&db=PubMed&dopt=Citation&list_uids=11837797.
- Ehrhardt, M. R., Flynn, P. F., and Wand, A. J. (1999). Preparation of encapsulated proteins dissolved in low viscosity fluids. *J. Biomol. NMR* 14, 75-78. Available at: <http://www.ncbi.nlm.nih.gov/pubmed/10382308> [Accessed April 29, 2011].
- Fan, J. Q., and Ishii, S. (2007a). Active-site-specific chaperone therapy for Fabry disease. *FEBS Journal* 274, 4962–4971.
- Fan, J. Q., and Ishii, S. (2007b). Active-site-specific chaperone therapy for Fabry disease. Yin and Yang of enzyme inhibitors. *FEBS J* 274, 4962-71. Available at: http://www.ncbi.nlm.nih.gov/entrez/query.fcgi?cmd=Retrieve&db=PubMed&dopt=Citation&list_uids=17894781.
- Fervenza, F. C., Torra, R., and Warnock, D. G. (2008). Safety and efficacy of enzyme replacement therapy in the nephropathy of Fabry disease. *Biologics* 2, 823-43. Available at: http://www.ncbi.nlm.nih.gov/entrez/query.fcgi?cmd=Retrieve&db=PubMed&dopt=Citation&list_uids=19707461.

- Figura, K. V., and Hasilik, A. (2010). Lysosomal Enzymes and their Receptors. *Annu. Rev. Biochem.* 55, 167-193. Available at: <http://dx.doi.org/10.1146/annurev.bi.55.070186.001123>.
- Fujimoto, Z., Kaneko, S., Momma, M., Kobayashi, H., and Mizuno, H. (2003). Crystal structure of rice alpha-galactosidase complexed with D-galactose. *J Biol Chem* 278, 20313-8. Available at: http://www.ncbi.nlm.nih.gov/entrez/query.fcgi?cmd=Retrieve&db=PubMed&dopt=Citation&list_uids=12657636.
- Garman, S. C., and Garboczi, D. N. (2002). Structural basis of Fabry disease. *Mol Genet Metab* 77, 3-11. Available at: http://www.ncbi.nlm.nih.gov/entrez/query.fcgi?cmd=Retrieve&db=PubMed&dopt=Citation&list_uids=12359124.
- Garman, S. C., and Garboczi, D. N. (2004). The molecular defect leading to Fabry disease: structure of human alpha-galactosidase. *J Mol Biol* 337, 319-35. Available at: http://www.ncbi.nlm.nih.gov/entrez/query.fcgi?cmd=Retrieve&db=PubMed&dopt=Citation&list_uids=15003450.
- Granados, R., Guoxun, L., Derksen, A., and McKenna, K. (1994). A new insect cell line from *Trichoplusia ni* (BTI-Tn-5B1-4) susceptible to *Trichoplusia ni* single enveloped nuclear polyhedrosis virus. *Journal of Invertebrate Pathology* 64, 260-266. Available at: http://www.sciencedirect.com/science?_ob=ArticleURL&_udi=B6WJV-4F7S1Y8-J&_user=607017&_coverDate=11%2F30%2F1994&_rdoc=1&_fmt=high&_orig=search&_origin=search&_sort=d&_docanchor=&view=c&_searchStrId=1508250637&_rerunOrigin=scholar.google&_acct=C000031527&_version=1&_urlVersion=0&_userid=607017&md5=1d932a724ec83006500beac01b66f597&searchtype=a [Accessed October 21, 2010].
- Gravel, R. A., Lowden, J. A., Callahan, J. W., Wolfe, L. S., and Kin, N. M. N. Y. (1979). Infantile sialidosis: a phenocopy of type 1 GM1 gangliosidosis distinguished by genetic complementation and urinary oligosaccharides. *American Journal of Human Genetics* 31, 669.
- Guce, A. I., Clark, N. E., Salgado, E. N., Ivanen, D. R., Kulminskaya, A. A., Brumer, H., and Garman, S. C. (2010a). Catalytic Mechanism of Human α -Galactosidase. *Journal of Biological Chemistry* 285, 3625 - 3632. Available at: <http://www.jbc.org/content/285/6/3625.abstract> [Accessed April 3, 2011].
- Guce, A. I., Clark, N. E., Salgado, E. N., Ivanen, D. R., Kulminskaya, A. A., Brumer, H., and Garman, S. C. (2010b). Catalytic Mechanism of

Human α -Galactosidase. *Journal of Biological Chemistry* 285, 3625 - 3632. Available at: <http://www.jbc.org/content/285/6/3625.abstract> [Accessed April 3, 2011].

Harris, D. C. (2003). *Quantitative chemical analysis* (Macmillan).

Harzer, K., Cantz, M., Sewell, A. C., Dhareshwar, S. S., Roggendorf, W., Heckl, R. W., Schofer, O., Thumler, R., Peiffer, J., and Schlote, W. (1986). Normomorphonic sialidosis in two female adults with severe neurologic disease and without sialyl oligosacchariduria. *Human genetics* 74, 209–214.

Henrissat, B., and Davies, G. (1997). Structural and sequence-based classification of glycoside hydrolases. *Curr Opin Struct Biol* 7, 637-44. Available at: http://www.ncbi.nlm.nih.gov/entrez/query.fcgi?cmd=Retrieve&db=PubMed&dopt=Citation&list_uids=9345621.

Hsu, T., Takahashi, N., Tsukamoto, Y., Kato, K., Shimada, I., Masuda, K., Whiteley, E., Fan, J., Lee, Y., and Betenbaugh, M. (1997). Differential N-Glycan Patterns of Secreted and Intracellular IgG Produced in *Trichoplusia ni* Cells. *J Biol Chem* 272, 9062-9070. Available at: <http://www.jbc.org/content/272/14/9062.full> [Accessed October 21, 2010].

Hubbes, M., d'Agrosa, R. M., and Callahan, J. W. (1992). Human placental beta-galactosidase. Characterization of the dimer and complex forms of the enzyme. *Biochemical Journal* 285, 827.

Iakoucheva, L. M., and Dunker, A. K. (2003). Order, Disorder, and Flexibility: Prediction from Protein Sequence. *Structure* 11, 1316-1317. Available at: <http://www.sciencedirect.com/science/article/B6VSR-49YDS35-6/2/f98d91e4229ea219662f3f55436f0be6> [Accessed April 11, 2011].

Invitrogen Corporation (2008). Bac-to-Bac® TOPO® Expression System An efficient cloning and site-specific transposition system to generate recombinant baculovirus for high-level protein expression. Available at: <http://www.google.com/search?q=bac+to+bac+topo+expression+system+manual&ie=utf-8&oe=utf-8&aq=t&rls=org.mozilla:en-US:official&client=firefox-a> [Accessed April 7, 2011].

Ishii, S., Chang, H. H., Kawasaki, K., Yasuda, K., Wu, H. L., Garman, S. C., and Fan, J. Q. (2007). Mutant alpha-galactosidase A enzymes identified in Fabry disease patients with residual enzyme activity: biochemical characterization and restoration of normal intracellular

processing by 1-deoxygalactonojirimycin. *Biochem J* 406, 285-95.

Available at:

http://www.ncbi.nlm.nih.gov/entrez/query.fcgi?cmd=Retrieve&db=PubMed&dopt=Citation&list_uids=17555407.

Kashtan, C. E., Nevins, T. E., Posalaky, Z., Vernier, R. L., and Fish, A. J. (1989). Proteinuria in a child with sialidosis: case report and histological studies. *Pediatric Nephrology* 3, 166-174.

Linding, R., Jensen, L. J., Diella, F., Bork, P., Gibson, T. J., and Russell, R. B. (2003). Protein Disorder Prediction: Implications for Structural Proteomics. *Structure* 11, 1453-1459. Available at: <http://www.sciencedirect.com/science/article/B6VSR-49YDS35-P/2/3eda046e8f31c70bf47c616db051f0dc> [Accessed April 11, 2011].

Lopez, M. M., and Makhatadze, G. I. (2002). Isothermal Titration Calorimetry. In *Calcium-Binding Protein Protocols* (New Jersey: Humana Press), pp. 121-126. Available at: <http://www.springerlink.com/silk/library.umass.edu/content/g048t63381462732/#section=92387&page=1> [Accessed April 27, 2011].

MacDermot, J., and MacDermot, K. D. (2001). Neuropathic pain in Anderson-Fabry disease: pathology and therapeutic options. *Eur J Pharmacol* 429, 121-5. Available at: http://www.ncbi.nlm.nih.gov/entrez/query.fcgi?cmd=Retrieve&db=PubMed&dopt=Citation&list_uids=11698033.

MacDermot, K. D., Holmes, A., and Miners, A. H. (2001a). Anderson-Fabry disease: clinical manifestations and impact of disease in a cohort of 60 obligate carrier females. *J Med Genet* 38, 769-75. Available at: http://www.ncbi.nlm.nih.gov/entrez/query.fcgi?cmd=Retrieve&db=PubMed&dopt=Citation&list_uids=11732485.

MacDermot, K. D., Holmes, A., and Miners, A. H. (2001b). Anderson-Fabry disease: clinical manifestations and impact of disease in a cohort of 98 hemizygous males. *J Med Genet* 38, 750-60. Available at: http://www.ncbi.nlm.nih.gov/entrez/query.fcgi?cmd=Retrieve&db=PubMed&dopt=Citation&list_uids=11694547.

MacDermot, K. D., Holmes, A., and Miners, A. H. (2001c). Natural history of Fabry disease in affected males and obligate carrier females. *J Inher Metab Dis* 24 *Suppl* 2, 13-4; discussion 11-2. Available at: http://www.ncbi.nlm.nih.gov/entrez/query.fcgi?cmd=Retrieve&db=PubMed&dopt=Citation&list_uids=11758673.

- Maiorella, B. (1988). Large-Scale Insect Cell-Culture for Recombinant Protein Production. *Biotechnology* 6, 1406-1410. Available at: <http://www.google.com/> [Accessed November 18, 2010].
- Matsuda, J., Suzuki, O., Oshima, A., Yamamoto, Y., Noguchi, A., Takimoto, K., Itoh, M., Matsuzaki, Y., Yasuda, Y., Ogawa, S., et al. (2003). Chemical chaperone therapy for brain pathology in GM1-gangliosidosis. *Proceedings of the National Academy of Sciences of the United States of America* 100, 15912-15917. Available at: <http://www.pnas.org/content/100/26/15912.abstract> [Accessed November 29, 2010].
- Meikle, N. O. for R. (2003). *NORD guide to rare disorders* (Lippincott Williams & Wilkins).
- Meikle, P. J., Hopwood, J. J., Clague, A. E., and Carey, W. F. (1999). Prevalence of lysosomal storage disorders. *Jama* 281, 249.
- Naganawa, Y., Itoh, K., Shimmoto, M., Takiguchi, K., Doi, H., Nishizawa, Y., Kobayashi, T., Kamei, S., Lukong, K. E., Pshezhetsky, A. V., et al. (2000). Molecular and structural studies of Japanese patients with sialidosis type 1. *Journal of Human Genetics* 45, 241-249.
- Neufeld, E. F., Lim, T. W., and Shapiro, L. J. (1975). Inherited Disorders of Lysosomal Metabolism. *Annu. Rev. Biochem.* 44, 357-376. Available at: <http://www.annualreviews.org.silk.library.umass.edu/doi/abs/10.1146/annurev.bi.44.070175.002041> [Accessed March 4, 2011].
- O'Reilly, D., Miller, L., and Luckow, V. (1994). *Baculovirus Expression Vectors - A Laboratory Manual* 1st ed. (New York, Oxford: Oxford University Press).
- Phizicky, E. M., and Fields, S. (1995). Protein-protein interactions: methods for detection and analysis. *Microbiology and Molecular Biology Reviews* 59, 94.
- Royce, P. M., and Steinmann, B. U. (2002). *Connective tissue and its heritable disorders: molecular, genetic, and medical aspects* (John Wiley and Sons).
- Rudenko, G., Bonten, E., d'Azzo, A., and GJ Hol, W. (1995). Three-dimensional structure of the human protective protein: structure of the precursor form suggests a complex activation mechanism. *Structure* 3, 1249-1259. Available at: <http://www.sciencedirect.com/science/article/B6VSR-4CXD8P1->

49/2/1fb843604d2fd8b8c4084cd528981ddd [Accessed February 16, 2011].

Schiffmann, R. (2009). Fabry disease. *Pharmacol Ther* 122, 65-77. Available at:
http://www.ncbi.nlm.nih.gov/entrez/query.fcgi?cmd=Retrieve&db=PubMed&dopt=Citation&list_uids=19318041.

Schiffmann, R., Kopp, J. B., Austin, H. A., Sabnis, S., Moore, D. F., Weibel, T., Balow, J. E., and Brady, R. O. (2001). Enzyme replacement therapy in Fabry disease. *JAMA: The Journal of the American Medical Association* 285, 2743.

Settembre, C., Fraldi, A., Jahreiss, L., Spampinato, C., Venturi, C., Medina, D., de Pablo, R., Tacchetti, C., Rubinsztein, D. C., and Ballabio, A. (2008). A block of autophagy in lysosomal storage disorders. *Human Molecular Genetics* 17, 119 -129. Available at:
<http://hmg.oxfordjournals.org/content/17/1/119.abstract> [Accessed April 17, 2011].

Shabbeer, J., Yasuda, M., Benson, S. D., and Desnick, R. J. (2006). Fabry disease: identification of 50 novel alpha-galactosidase A mutations causing the classic phenotype and three-dimensional structural analysis of 29 missense mutations. *Hum. Genomics* 2, 297-309. Available at: <http://www.ncbi.nlm.nih.gov/pubmed/16595074> [Accessed April 26, 2011].

Siamopoulos, K. C. (2004). Fabry disease: kidney involvement and enzyme replacement therapy. *Kidney international* 65, 744–753.

Skerra, A., and Schmidt, T. G. M. (1999). Applications of a peptide ligand for streptavidin: the Strep-tag. *Biomolecular Engineering* 16, 79-86. Available at: <http://www.sciencedirect.com/science/article/B6VRM-3Y51GKM-C/2/a9da07ff2ca24bd97acf946a5ca73b77> [Accessed April 7, 2011].

Sons, J. W. & (2002). Wiley encyclopedia of molecular medicine (John Wiley).

Swallow, D. M., Evans, L., Stewart, G., Thomas, P. K., and Abrams, J. D. (1979). Sialidosis type 1: cherry red spot-myoclonus syndrome with sialidase deficiency and altered electrophoretic mobility of some enzymes known to be glycoproteins. II. Enzymes studies. *Ann. Hum. Genet* 43, 27-35. Available at:
<http://www.ncbi.nlm.nih.gov/pubmed/496393> [Accessed November 28, 2010].

- Tobimatsu, S., Fukui, R., Shibasaki, H., Kato, M., and Kuroiwa, Y. (1985). Electrophysiological studies of myoclonus in sialidosis type 2. *Electroencephalography and clinical neurophysiology* 60, 16–22.
- Valentine, K. G., Pometun, M. S., Kielec, J. M., Baigelman, R. E., Staub, J. K., Owens, K. L., and Wand, A. J. (2006). Magnetic Susceptibility-Induced Alignment of Proteins in Reverse Micelles. *Journal of the American Chemical Society* 128, 15930-15931. Available at: <http://dx.doi.org/10.1021/ja061438n> [Accessed April 29, 2011].
- Varki, A. (1999). *Essentials of glycobiology* (Cold Spring Harbor Laboratory Pr).
- Wang, R. Y., Lelis, A., Mirocha, J., and Wilcox, W. R. (2007a). Heterozygous Fabry women are not just carriers, but have a significant burden of disease and impaired quality of life. *Genetics in Medicine* 9, 34-45. Available at: http://journals.lww.com/geneticsinmedicine/Abstract/2007/01000/Heterozygous_Fabry_women_are_not_just_carriers,6.aspx [Accessed April 13, 2011].
- Wang, R. Y., Lelis, A., Mirocha, J., and Wilcox, W. R. (2007b). Heterozygous Fabry women are not just carriers, but have a significant burden of disease and impaired quality of life. *Genetics in Medicine* 9, 34-45. Available at: http://journals.lww.com/geneticsinmedicine/Abstract/2007/01000/Heterozygous_Fabry_women_are_not_just_carriers,6.aspx [Accessed April 13, 2011].
- Warren, L. (1959). Sialic acid in human semen and in the male genital tract. *J Clin Invest* 38, 755-761.
- Wickham, T., Davis, R., Granados, R., and Shuler, M. (1992). Screening of insect cell lines for the production of recombinant proteins and infectious virus in the baculovirus expression system. *Biotechnol. Prog.* 8, 391-396. Available at: <http://pubs.acs.org/doi/abs/10.1021/bp00017a003> [Accessed October 21, 2010].
- Wilcock, B. (2009). *Pharmacological Chaperone Therapy*. Available at: www.scs.illinois.edu/burke/files/group_meetings/bcw_575abstract.pdf.
- Winter, R. M., Swallow, D. M., Baraitser, M., and Purkiss, P. (1980). Sialidosis type 2 (acid neuraminidase deficiency): clinical and biochemical features of a further case. *Clinical genetics* 18, 203–210.

- Yam, G. H., Zuber, C., and Roth, J. (2005). A synthetic chaperone corrects the trafficking defect and disease phenotype in a protein misfolding disorder. *FASEB J* *19*, 12-8. Available at:
http://www.ncbi.nlm.nih.gov/entrez/query.fcgi?cmd=Retrieve&db=PubMed&dopt=Citation&list_uids=15629890.
- Yamamoto, Y., and Nishimura, K. (1987). Copurification and separation of [beta]-galactosidase and sialidase from porcine testis. *International Journal of Biochemistry* *19*, 435–442.
- Yan, S. and G. W. (2009). Mutation patterns in human α -galactosidase A. *Mol Divers* *10*, 11030-991584.